Exposure of the population of southern France to air pollutants in future climate case studies

Arineh Cholakian, Isabelle Coll, Augustin Colette, Matthias Beekmann

HAL Id: ineris-03500551

https://ineris.hal.science/ineris-03500551

Submitted on 23 Dec 2021

Contents lists available at ScienceDirect

Atmospheric Environment

journal homepage: www.elsevier.com/locate/atmosenv
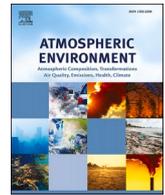
Exposure of the population of southern France to air pollutants in future climate case studies

Arineh Cholakian [a,b,c,*,1], Isabelle Coll [a], Augustin Colette [b], Matthias Beekmann [c]

[a] Univ Paris Est Creteil and Université de Paris, CNRS, LISA, F-94010 Créteil, France
[b] Institut National de l'Environnement Industriel et des Risques, Parc Technologique ALATA, Verneuil-en-Halatte, France
[c] Université de Paris and Univ Paris Est Creteil, CNRS, LISA, F-75013 Paris, France

HIGHLIGHTS

- Clarification on the fact that we have chosen to perform case studies and not future scenarios
- Clarification on the choice made for the years simulated and the method used for this choice
- Organization of the sections: separating results from the methodology
- Adding references to corroborate several points raised by the reviewer
- Changes to the visibility of the axes in the images
- Some general proof-reading changes
- Clarification on the county-per-county analysis

ARTICLE INFO

ABSTRACT

Population exposure to air pollutants varies dramatically with time and location on the globe. Taking into account the changing climate, the engaged emission reduction policies and the expected increase in population, the health risks associated with this phenomenon may also change significantly in the near future. In regions such as the Mediterranean, exposed to multiple forms of air pollution and highly sensitive to climate change, it is obviously critical to define trends in human exposure to air pollutants. The objective of this article is to explore the features of population exposure to air pollution in the French Mediterranean coast, under different climatic situations, using distinct emission configurations, and for divergent scenarios of population growth. The use of contrasting situations for these 3 parameters makes it possible to better address the variability of exposure in the different areas of the territory, as a global risk for populations. For this purpose, five 12 month-duration simulations have been carried out as case studies in the Provence Alpes Côtes d'Azur (PACA) region, located in the south-east of France: a 2005 simulation is used as the reference situation, and two more years of simulation are used as samples of time horizons 2030 and 2050, each of which was simulated twice sampling representative future climate years according to representative concentration pathway scenarios RCP4.5 and RCP8.5. Estimates of population change were prepared for the study area, using shared socioeconomic pathways (SSPs) scenarios. The results show that albeit the growing population, the exposure to most atmospheric components decreases because of emission reduction policies. This, however, is not true for all species. The population exposure to dust species increases for spring, when most dust episodes occur. In addition, exposure to ozone – while decreasing on the average - shows an increase in urban areas. Finally, while the concentrations of BSOA (secondary organic aerosol of biogenic origin) increase in the future scenarios, this tendency is not marked enough to offset the population decrease in rural areas in most SSP scenarios. On the reverse, exposure to BSOA does show an increase in urban areas where population is expected to grow. A county per county analysis is conducted, showing that the three coastal counties of the PACA region will experience higher ozone, PM_{10} and $PM_{2.5}$, dust and BSOA exposure. The purpose of our work is to produce a case study in which we compare pollutant concentration changes and population weighed exposure changes on a

meteorological situation that goes out of the current distribution. For this case study, we propose to distinguish the part of exposure changes due pollutant concentration and population changes. The choice of the study case (weather and horizon) is discussed in the text. This approach differs from the scenario approach, which focuses on the analysis of a trend representative of future years.

1. Introduction

Air quality and climate are intertwined in their effects and their changes, meaning that as a result of mitigating climate change, air quality will improve as well and vice-versa (Jacob and Winner, 2009). Of course, this implies that the climate change mitigation strategy includes an indirect reduction of emission of anthropogenic pollutants into the atmosphere. We already know that atmospheric pollutants can have adverse effects on human health (Pope and Dockery, 2006; Mauderly and Chow, 2008; Anderson et al., 2012). These health effects have been also evaluated for particulate matter, showing that they can, among other conditions, cause commonly cardiovascular diseases such as heart attacks and even more frequently pulmonary diseases ranging from asthma to lung cancer, depending on the size of the particles which determines their depth of penetration into the lungs (Harrison and Yin, 2000). There are also studies suggesting that certain species of PM (specifically dust particles) in addition to the normal cardiovascular effects (De Longueville et al., 2010; Middleton, 2017) can also contribute to the transfer of viral, fungal and bacterial diseases, since some types of these microorganisms are capable of surviving long distance transport (Griffin, 2007). Therefore, mitigation efforts to combat climate change may also help reduce health problems related to exposure to air pollution. However, the very effects of climate change can lead to an exacerbation of emission phenomena, or favor photochemical processes. A future worsening of air quality might be due to (i) increased dust emissions, as a result of drought and land use changes (Mahowald et al., 2010; Mulitza et al., 2010; Lee and Sohn, 2011), (ii) elevated levels of ozone in the atmosphere due to reduced NO_x titration, faster production rates or increased biogenic precursor emissions (Colette et al., 2015; Fortems-Cheiney et al., 2017; Cholakian et al., 2019a), the latter also affecting secondary organic aerosols. Therefore, the analysis of air quality in distant horizons should not only rely on the implementation of emission control and low-carbon policies, but also consider the meteorological expression of climate change.

Such an analysis must also be based on indicators that can be more directly related to health risks, and that integrate more parameters than pollutant concentrations do. Indeed, since the environmental risk is calculated as a cumulative impact on the health of the entire population, the population increase is indeed a mechanical lever to increase the overall risk. Thus, although exposure to atmospheric particles reaches quite high levels in deserts and coastal areas due to the emissions of terrigenous dust and the presence of sea salt, it does not affect the exposure risk, which remains the highest in the world in China and India due to the combination of high population density and elevated pollution levels (Kan et al., 2012; van Donkelaar et al., 2015). Therefore, in the context of climate change, the future impacts of air quality on human health must be assessed by calculating the total population exposure in a given region, taking into account the demographic evolution of this region. In particular, increasing urban population can lead to a redistribution of health issues related to air quality, including local increase of the risk of exposure to primary pollutants in urban areas. As demographic developments may show different features according to socio-economic conditions, scenarios using societal and environmental data should be considered to allow accurate estimates of population growth, aging and distribution across a territory. Such a work has been done for the European area by Tarín-Carrasco et al. (2021), pointing out that the premature mortality is highly correlated with the aging of the population.

Finally, there remains the question of the scale at which air quality simulations must be conducted to produce a relevant analysis of population exposure. Numerous studies have already explored the inter-related effects of emissions control and climate change on air quality, using either global or continental-scale chemistry-transport models. Global models have the advantage of dealing with the Earth system as a whole (Hauglustaine et al., 2014), simulating the connections between global and synoptic meteorological phenomena, and the interactions of the atmosphere with the continental and ocean surfaces. Thus, they can produce estimates of future concentration fields taking into account the multiple drivers of climate change. Continental scale models also have the advantage of being able to take into consideration the transport of air masses over long distances, and to integrate the impact of all sources of gaseous or particulate atmospheric compounds along their path. However, none of them can reproduce fine scale phenomena such as those related to the local topography, or to the heterogeneity of human emitting activities, since for each grid-cell they provide an averaged concentration value that doesn't account for small-scale processes. While it is obviously necessary to have a global vision of atmospheric processes and their consequences, this is not always sufficient to model actual exposure to air pollution as the geography of a site, the local meteorological phenomena, the distribution of human activities and the gradients of population density are needed to produce a better integration of risk across rural and urban areas. Thus, chemistry transport models implemented at high horizontal and vertical resolution and forced by highly resolved data, even on a limited area, provide a more detailed simulation of atmospheric chemistry in complex terrain, and a more realistic representation of concentration field gradients around urban areas. Yet, future climate modeling studies conducted at a high-resolution domain are not reported often in the literature. Therefore, we have decided to conduct a fine-scale study by simulating the exposure of the population on a high-resolution domain over a restricted area, nested into a coarser domain covering a larger area. To the best of our knowledge, these types of studies for this region are not commonly abundant in the literature, especially when exposure of the population and future scenarios are coupled.

This work specifically focuses on air pollution exposure in the Mediterranean area, a region for which the impacts of climate change are expected to be critical. Indeed, not all regions have the same sensitivity to climate change. Some regions can show higher response to a changing climate because of their particular atmospheric and geographic characteristics. Giorgi (2006) calculated a sensitivity factor for climate change depending on precipitation and temperature changes for wet and dry seasons for different regions of the world, concluding that the sensitivity for some regions is much higher than the other ones. In his study, the Mediterranean basin and the north-eastern European region are shown to be more sensitive to climate change than the other studied areas (the study excluded the arctic). Other studies have arrived to the same conclusion as well (Adloff et al., 2015; Ciardini et al., 2016). The Mediterranean region has particulate characteristics, such as presence of orographically high land on its continental surroundings, the longer than usual residence time of atmospheric compounds, the high photochemical potential or the accumulation of local and transported emissions (Lelieveld et al., 2002). Therefore, it is an area in which exposure to pollutants is forced by the geographical configuration, the intensity of solar radiation and the local dynamics of air masses, and therefore, since it has already been shown in the literature that this region is going to experience higher sensitivity to climate change, the Mediterranean can experience a possible exacerbation of a drop in air quality in the future.

Despite this, the future health impacts of air quality in the

Mediterranean region are still partially undetermined. Samoli et al. (2013) explored 10 cities in the Mediterranean region, investigating the particulate matter related mortality for each one. They found that there is a strong correlation between PM2.5 concentrations and air pollution related mortality. The exposure seen in this study is consistent to other city-scaled exposure studies for the US and Europe. The evolution of the composition of the atmosphere –and especially its aerosol content – is therefore critical for this region. However, although studies such as West et al. (2013) found a decrease in future exposure to ozone and PM2.5 at the global scale, few authors investigated the trends of exposure to air pollutants in the Mediterranean basin. This is why we have chosen to focus our study on the provision of new diagnoses on the evolution of air quality in the south of France, on the shores of the Mediterranean. Our target region, called PACA region (Provence Alpes Côtes d'Azur), has a high density of population linked with the presence of multiple urban ports on its coastal boundaries. It has been known for having serious air pollution problems because of high rates of urban and industrial emission and elevated temperature (Sicard et al., 2010). Very high concentrations of PM_{10} have been found in the region using satellite data (Péré et al., 2009). Furthermore, the PACA region is a high-risk area for dust episodes, which constitutes a supplementary concern for human health. A study conducted with the CHIMERE model confirmed the importance of implementing ambitious emission control policies in the area to control oxidizing pollution events (Coll et al., 2009). The combination of demographic and climate scenarios is now needed to provide quantified information on the potential risk of exposure of urban and rural population to air pollution, as well as its sensitivity to climatic factors and emission control strategies.

In this work, we simulated case studies of air quality and population exposure for several scenarios of changes in anthropogenic emissions and climate change (RCP4.5 and RCP8.5) in France, on the southern shores of the Mediterranean. In addition to a baseline year, two years representing respectively the 2030 and 2050 horizons were selected and simulated for each of the two RCP scenarios above. These two years selected have an average annual temperature higher than the median of the distribution over the decade concerned. This choice should make it possible to explore situations with a high impact of climate change on exposure. The simulations were first performed for the European domain, then for a nested domain corresponding to the PACA region - this with a high (5 km) horizontal resolution. The population changes for this region have been estimated from shared socioeconomic pathway (SSP) scenarios, from which the exposure of the current and future population and its changes are discussed.

In the following sections, a brief description of the simulation process is given, then the generation of current and future anthropogenic emissions and population scenarios for the PACA region is explained. Section 4 presents a general assessment of changes in air quality over the studied region, while exposure and its evolution are explored in section 5. Finally, a conclusion on the results of our study is proposed in the last section.

2. Materials and methods

This section provides a brief introduction to the operating principles of the chemistry-transport model (CTM) CHIMERE. The input data used for this study are detailed, in particular the specific inputs used for the high-resolution domain. Finally, the data used for the 2D representation of the current population of the PACA region are presented, and the choice of demographic trends for 2030 and 2050 are discussed.

2.1. CHIMERE CTM

The CHIMERE CTM (Menut et al., 2013) has been used in many studies across Europe and also in other parts of the world, both for research and operational forecasting purposes. Like all CTMs, CHIMERE needs input information in order to perform simulations for a specific

region: boundary conditions, meteorological fields, anthropogenic and biogenic emissions as well as chemical reactions and their associated rates have to be provided for the model to operate. Dust emissions are also considered in the model. For African dust emissions, we used the parameterization suggested by Alfaro and Gomes (2001) and the optimizations from Menut et al. (2005). The model proposed by Alfaro and Gomes (2001) is the combination of the saltation flux calculation proposed by Marticorena and Bergametti (1995) and the sandblasting model by Alfaro et al. (1998). For European dust emissions the model follows the method proposed by Zender et al. (2003). Fire emissions can be included in the CHIMERE model as well, but they have not been taken into account in this work because its future evolution was considered as too speculative in this work, depending not only on change in climate variables, but also on forest management practices. For its operation, CHIMERE includes modules that treat horizontal and vertical transport, atmospheric chemistry, formation and size distribution of aerosols and deposition, each one of these parameters being calculated in parallel mode using the related input information. The aerosols simulated in the default version of the model include elemental carbon (EC), sulfate, nitrate, ammonium, SOA (secondary organic aerosols, detailed in the next section), dust, salt and PPM (primary particulate matter other than ones mentioned above). The aerosol module takes into account coagulation, nucleation and absorption; and wet and dry deposition are treated by the deposition module. A sectional logarithmic size distribution is used for the speciation of aerosols into different size bins. More information on the default chemical mechanism, details for the reactions and their kinetic constants are given in Menut et al. (2013).

2.2. Simulations

For a domain covering the entire Europe it would be numerically heavy to use a horizontal resolution that is appropriate for an urban scale (5 km or less). Therefore, the nesting option can be used. In this study, two domains are used: the coarse domain covering continental Europe with a resolution of 0.44° and the nested domain focusing on the PACA region with a horizontal resolution of 5 km being forced by the initial and boundary conditions of the coarse domain (domains shown in Fig. 1). The vertical resolution for both domains is 9 levels ranging from the surface to 500 mb. For aerosols, 10 size distribution bins are used, ranging between 40 nm and 40 μm.

Meteorological fields are taken from the IPSL WRF member of EURO-CORDEX (Jacob et al., 2014) project for both domains; for the coarse domain we used fields with a horizontal resolution of 0.44°, while for the fine domain, more detailed meteorological simulations with a horizontal resolution of 10 km have been used. Biogenic emissions are provided to CHIMERE by the Model of Emissions of Gases and Aerosols from Nature (MEGAN, Guenther et al., 2006): they include isoprene, limonene, α-pinene, β-pinene, ocimene and other mono-terpenes with a base horizontal resolution of 0.008 × 0.008°. As CO_2 emissions have a limiting effect on isoprene emissions (HEALD et al., 2009; Tai et al., 2013), the inhibition of isoprene emissions by CO_2 has been added to MEGAN using the parameterization from Wilkinson et al. (2009). Boundary/initial conditions are provided by the LMDZ-INCA global model, specifically ran for the climate scenario used in each test case.

The Mediterranean region presents some challenges when it comes to the simulation of organic aerosols (OA). Most of the biogenic OA existing in the Mediterranean atmosphere is transported from the continental Europe towards the basin, since there are no emissions of precursors for this species at the sea surface. Furthermore, it has been observed that the biogenic OA in the region accounts for the majority of OA, especially during summer. Therefore, since the possibility of aged OA being moved from the continent towards the basin is higher, it is important to integrate a scheme that takes into account the OA aging. This is why we have been modifying the representation of OA in the version of the model used for this study, in order to better account for the specificities of the Mediterranean region. It is based on the VBS (volatility basis set)
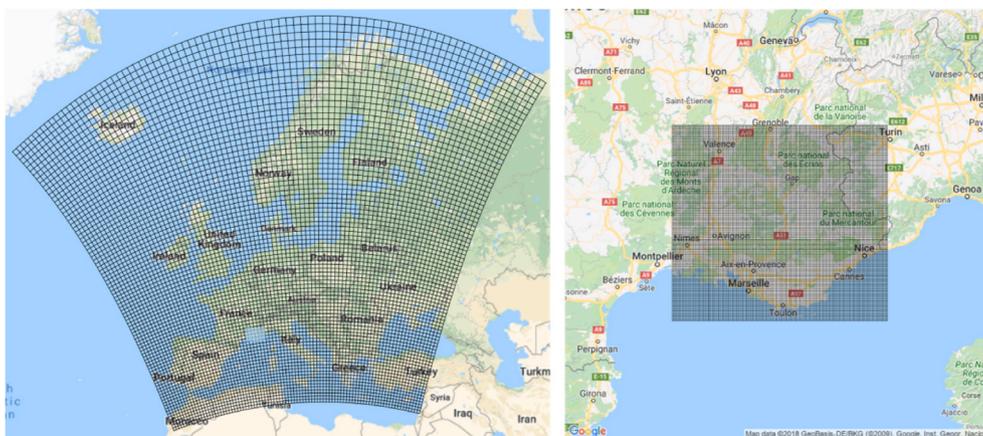
Fig. 1. Domains used in this study. Left: coarse domain with a horizontal resolution of 0.44°. right: nested domain with a horizontal resolution of 5 km.

scheme, which was first proposed by Robinson et al. (2007), and which distributes the organic aerosols in several volatility bins using the saturation concentration (C*), ranging from 10^{-2} μg m^{-3} to 10^6 μg m^{-3}. In this scheme, the aging processes for biogenic secondary organic aerosols (BSOA) and anthropogenic secondary organic aerosols (ASOA) are taken into account, as well as the emissions of intermediary volatile organic compounds (IVOC) and semi-volatile organic compounds (SVOC). Shrivastava et al. (2013, 2015) proposed some modifications to this scheme, adding fragmentation and formation of non-volatile SOA to the normal VBS scheme. In our study, this last version of VBS has been implemented in the CHIMERE model. The scheme has been previously tested for the Mediterranean region, for the year 2013, using the data obtained during the ChArMEx campaign for two in situ sites (Cap Corse and Mallorca). In this configuration, CHIMERE showed good agreement with the observed mass concentration and oxidation state of the organic aerosol (comparisons performed using the results of the PMF method) and with the origins of this aerosol (comparisons performed using the results of the ^{14}C measurements) for both sites mentioned above. A detailed explication of this validation is given in Cholakian et al. (2018). Also, the model configuration was validated over Europe for around 30 stations, as Cholakian et al. (2019b) found an overall good performance for this scheme, despite some underestimation during winter.

Our work is based on the simulation of 5 target years: one historic year reference year corresponding to the current situation, and four future case studies based on 2030 and 2050 timeframes. The year 2005 was chosen for the baseline simulation and the years 2033 and 2053 were used for the future test cases, as they showed - for the coarse European domain - higher than average temperature increases for the periods 2026 to 2035 and 2046 to 2055, respectively. These years were chosen by plotting the temperature distribution of both decades in the climate runs performed for the European domain, the years representing the 70% quantile were chosen. For each of those future timeframes, two distinct situations corresponding to representative concentration pathways (RCPs, Meinshausen et al., 2011), RCP4.5 (Thomson et al., 2011) and RCP8.5 (Riahi et al., 2011) have been simulated, according to the CMIP5 IPCC (IPCC, 2014) report.

2.3. Anthropogenic emissions

For the coarse domain, emissions provided by ECLIPSE-v4 (Amann et al., 2013; Klimont et al., 2017) have been used. For the historic simulation, baseline emissions of 2010 are used, while current legislation emissions (CLE) for 2030 and 2050 are assigned to the future scenarios. However, the base resolution of the ECLIPSE inventory is 0.5°, which is too coarse for our nested domain. Therefore, local bottom-up emissions dedicated to daily air quality forecasting were collected from the PACA air quality network (AtmoSud, https://www.atmosud.

org/), with a base resolution of 1 km. It is important to notice that these emissions correspond to the current period. Thus, 2030, 2050 emission projections have been calculated using the ECLIPSE emission ratio between the reference year and each of the two CLE scenarios, in order to ensure consistency between the coarse domain and the nested domain, on the specific point of the evolution of anthropogenic emissions.

Since the emissions provided by the AtmoSud network are defined on an irregular domain (shapefiles), a formatting process chain was carried out: it consisted of distributing the emissions on a 2D network and re-gridding them on a mesh useable in CHIMERE. Furthermore, AtmoSud emissions being limited to the administrative borders of the PACA region, a third necessary step of our formatting work was to fill the sides of the irregular domain with information provided by a complementary emission inventory (here MACC-III emissions for the same year, with a base resolution of 7 km, Kuenen et al., 2014). Finally, the obtained kilometric anthropogenic emissions had to be aggregated to fit the 5 km-resolution domain that will be used in our simulations. These steps are illustrated in Fig. 2. The emissions corresponding to the scenarios CLE 2030 and 2050 were then calculated from this inventory, using the evolution factors observed on the ECLIPSE inventory, as explained above. As the ECLIPSE inventory provides details of emissions by SNAP sectors (Selective Nomenclature for Air Pollution) for all listed species, evolution factors from 2010 baseline emissions to either CLE 2030 or CLE 2050 emissions were estimated for each snap sector in the PACA region, and applied to the AtmoSud inventory.

2.4. Current and future population for the PACA domain

The current population of the PACA region was calculated by LCSQA (Central Air Quality Monitoring Laboratory, LCSQA, 2015) on the same domain as that used for the current PACA emissions with a resolution of 1 km. So, the same projection and re-gridding procedure was conducted in order to obtain a population density dataset compatible with CHIMERE outputs. The results are shown in Fig. 4-a.

As described in Jones and O'Neill (2016) and O'Neill et al. (2017) several scenarios may be considered for the projection of population density, in order to consider different possible trends for population growth and urbanization. In our study, estimates of the future population density in the PACA region were derived from shared socioeconomic pathways (SSPs) provided at an initial resolution of 0.125°. The scenarios, which are described below, were compared to current situation provided by the same authors for the PACA region, and the factors of differences were applied to the current population density of the PACA region in order to get the 2030 and 2050 population scenarios.

SSPs are future scenarios that take into account energetic, economic and land use changes as well as emissions and radiative forcing changes.
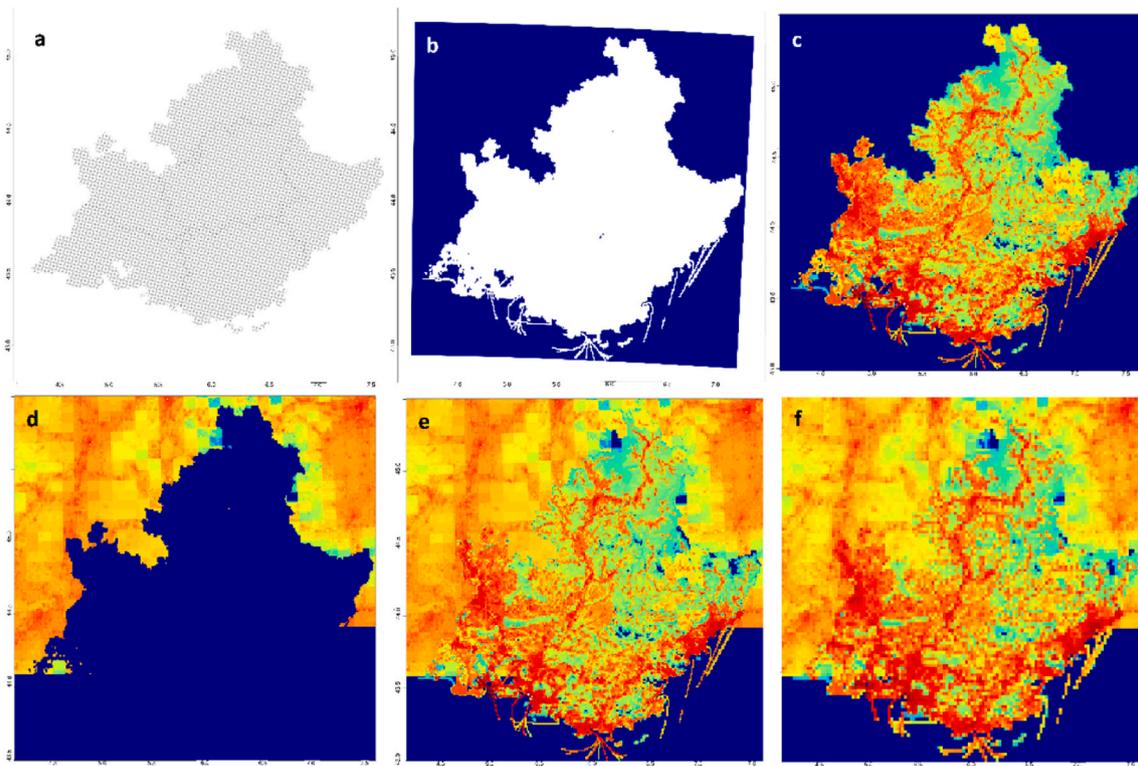
Fig. 2. The procedure of preparation of anthropogenic emissions for the PACA region (here shown the emissions of NO. a: the irregular domain the data was provided on. b: the same domain as a, but distributed regularly on a lambert domain. c: anthropogenic emissions distributed for the PACA region, projection changed from lambert to lan/lot. d: Same as c, but the exterior part of the domain is filled with MACC-III emissions. e: the panels c and d combined to provide the desired results in a 1k horizontal resolution, f: Same domain as d, re-gridded on a 5 km horizontal resolution.

There are five SSP scenarios, each based on a different possible narrative of alternative socio-economic development (Riahi et al., 2017). The population change in each scenario has been projected using mortality, fertility and migration parameters, while urbanization has been estimated only by using current fertility and income conditions. In each scenario there are two concepts that can change: global response to mitigation and to adaptation. All five SSP scenarios will be explained in this section, with an explication of what each of these scenarios could mean for the French population. At the end, a choice of two scenarios will be done in an effort to present the extreme future possibilities for France. The population change trends in SSPs for France are shown in Fig. 3.

SSP1 accounts for the sustainability trend, where environmental boundaries are respected and where the world moves slowly towards low resource and low energy use, also leading reduced inequalities between and within countries. This scenario assumes that there will be low challenges for the sustainable way of life and seems excessively

optimistic. In this scenario, population growth seems to slow down in high fertility countries because of more investment in education and health care. High but constrained urbanization is envisioned in this scenario. As for total population, it shows an increase until the 2040s and then starts to follow a decreasing pattern, while urbanization still increases till the end of the century. This scenario assumes low challenges for both mitigation and adaptation.

SSP2 is the "middle of the road" scenario. In this scenario, the patterns of economic and technological growth follow the historical trends: some countries progress very well while others do not. Therefore, inequalities still exist between countries. Finally, international development goals (in economy, renewable energy usage, population stabilization, etc.) are achieved but much more slowly than anticipated. Population increases till the 2070s and then shows a decreasing pattern. Urbanization is moderate in this scenario but it continues till the end of the century. It assumes medium challenges for mitigation and adaptation.

SSP3 is a regional rivalry scenario. Nationalism becomes more important than globalization, conflicts between countries and regions are likely and the policies become more oriented towards national or regional defense than environmental concerns. Economic development is slow and inequalities between countries increase over time. While environmental degradation worsens in many regions, no priority is given to this issue. Population as well as urbanization continue to increase until the end of the century, although the urbanization growth rate is lower compared with the other scenarios. This is a scenario where mitigation and adaptation become extremely difficult.

SSP4 can be defined as an "inequality scenario". It is somewhat similar to SSP3 in terms of slow economic and technological change. The difference between the two is the widening gap of inequalities both country-wide and between different countries, and conflicts become common. Inequalities both in economic opportunities and political power divide the world into two groups: the population majority in bad
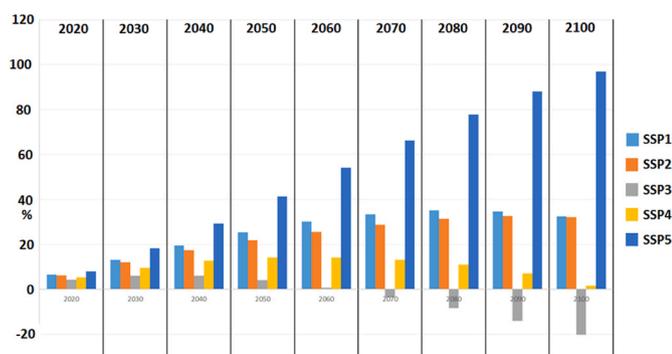
Fig. 3. Population change (in %) in all SSP scenarios for France, compared to 2005.
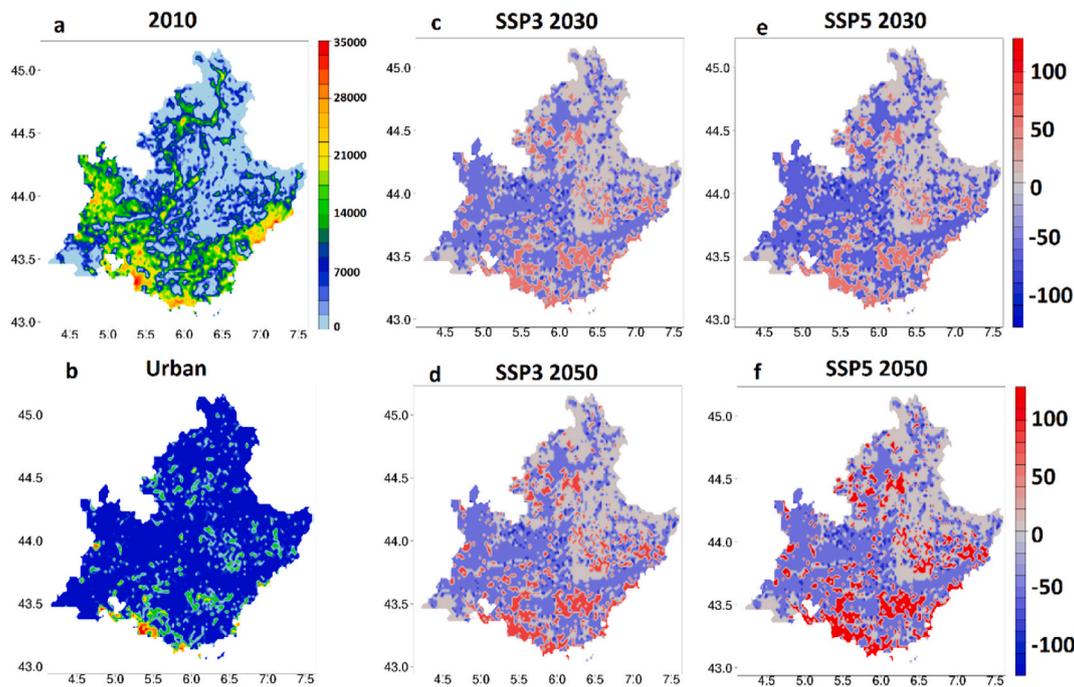
Fig. 4. Re-gridded population for 2005 (a) and its changes in future SSP3 and SSP5 demographic scenarios for 2030 timeframe (first row) and 2050 timeframe (second row) for the PACA region. Panel b shows the urban land use area in the PACA region.

economic conditions and the elite in power. Environmental concerns are treated regionally, in areas where the populations with high income reside. Population in this scenario grows until the 2070s before starting to decrease. Urbanization is strong and comparable to that of SSP1. Mitigation presents low challenges because of the power disparity while adaptation is extremely difficult.

SSP5 is the fossil-fuelled development scenario. In this scenario, the global market remains important and an increasing faith is placed on innovation and participatory societies that encourage fast technology and develop human capital (increased healthcare and education, etc.). These improvements however are performed using fossil fuel and the energy use around the world is intensive. Local environmental problems are solved rapidly, while global ones still remain. The population in this scenario starts decreasing in the 2040s and follows this trend until the end of the century. Urbanization however shows an increase similar to SS1 and SSP4. As expected, mitigation is assumed to be difficult for this scenario, while adaptation challenges are low.

The changes in population induced in each country by a given scenario may be different, due to national specificities such as fertility, mortality, migration and income. France is ranked among the high-income countries (Bank World, 2017), and its gross domestic product (GDP) shows an increasing trend in all SSP scenarios. On this basis, an increase in the population is predicted for SSP1 and SSP2 until the 2050s, and for SSP3 and SSP4 until the 2080s, before decreasing slightly (Fig. 3). In 2100, the SSP3 scenario even results in a lower total population than in 2020. SSP5, on the other hand, predicts a continuous increase of the French population until the end of the century. It is interesting to note that the share of urbanization (i.e. the urban to total population ratio) increases in all scenarios for high-income countries, and can reach as high as 95% by 2100.

In order to study the widest range of exposure variation in the PACA region, we therefore chose to focus our air quality analysis on the SSP3 and SSP5 scenarios, with SSP3 experiencing less population growth and urbanization, in a context of global conflicts and large regional inequalities, and SSP5 showing the highest population growth and the largest urbanization for the region. Thus, although all the demographic scenarios have been simulated, we will only detail here the results

obtained with the SSP3 and SSP5 projections. The resulting population changes, when compared with the reference simulation, are shown in Fig. 4 (panels c through f). In summary, in the PACA region, the population decreases in SSP3 in the 2030s and continues to do so until the 2050s. This decrease of population happens in rural areas, urban areas showing an increase in population for this scenario. For SSP5, population decreases in the 2030s, and shows an increase in the 2050s, the rural/urban changes of this population change remain similar to SSP3.

It is important to keep in mind that, although the Eclipse anthropogenic emissions already take into account future demographic changes. SSP scenarios are needed in this work as a best available scenario on future population changes need for exposition calculation. It might also be interesting to keep in mind that while RCPs and SSPs are different sets of future scenario types and were conceived to be complementary of each other, RCP8.5 and SSP5 are quite consistent with each other since both represent a "business as usual" type of scenario.

3. Results

In this section, a thorough analysis of the changes in the meteorological situation between 2005 and the future climatic case studies - as well as a comparative analysis of the simulated chemical concentration fields - is presented as a first step in the analysis of pollutant exposure maps for each future situation.

3.1. Meteorological parameters

Fig. 5 shows box plots of changes in the main simulated meteorological parameters (temperature, wind speed, relative humidity, height of the boundary layer, amount of precipitation and number of rainy hours) between the reference simulation and our prospective case studies. Changes with respect to the regional averages of the historical (2005) period are indicated, so that the box plots show the local spatial climate variability. It is important to keep in mind that the simulations are conducted for different years having their own meteorological specificities, so the inter-annual variability adds to the average impact of the scenario.
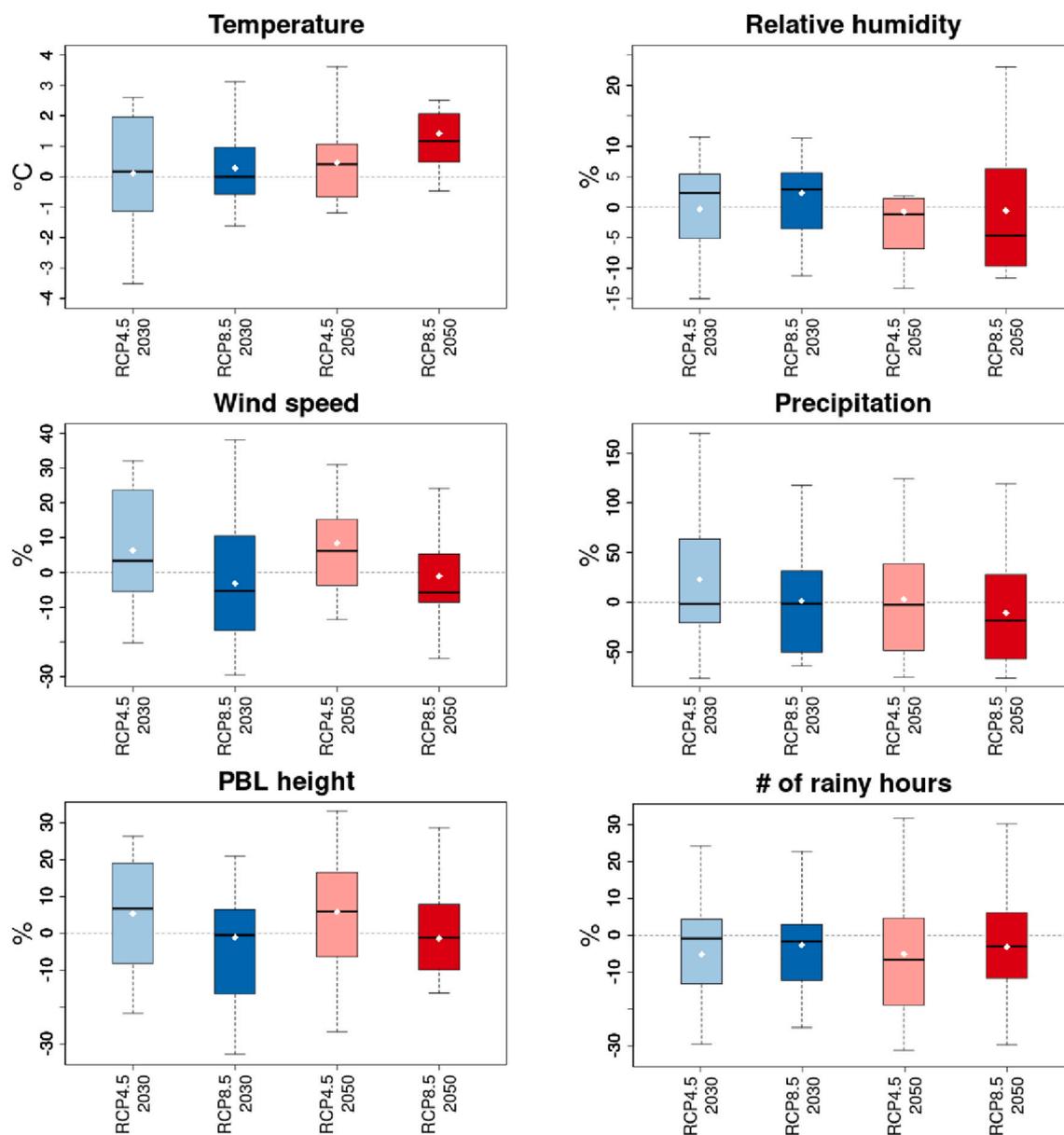
Fig. 5. Changes of meteorological parameters in future scenarios compared to historic simulation for 2005. The values are shown in percentage, except for temperature for which the delta in °C is shown. The boxplots are standard boxplots, the white spot on each boxplot shows the average for each one, the name of the scenarios is given on the x-axis of each grid. The dotted line shows the 0 reference.

Fig. 5 shows changes in average temperature between the 2005 reference simulation and the future case studies. They are small for the 30-RCP4.5 and 30-RCP8.5 scenarios, below 0.1 °C, +0.3 °C for the 50RCP8.5 scenario, and largest for the 50-RCP8.5 scenario, showing a temperature increase of 1.4 °C. Conversely, relative humidity remains on average rather unchanged between the different situations (modifications below 3%), but the median relative humidity and show a stronger decrease (−6%) and the variability is strongest in 50-RCP8.5. Similarly, the average amount of precipitation only shows slight changes from the historic to all the target years (with exception of 50 RCP-8.5), although a large increase is observed in the highest percentiles of all future simulations.

The average number of rainy hours keeps on the average again rather unchanged with stronger decreases in the 30-RCP4.5 and 50 RCP4.5 scenarios (−5%). Average 10m wind speed and boundary layer height most strongly increase for the 30-RCP4.5 50-RCP4.5 scenarios, by respectively (+5 to +9%) and (+5–6%). As a conclusion, largest temperature increase is observed for the 50-RCP8.5 scenario and is

correlated to decreases in relative humidity (median), precipitation, and wind speed.

This study should be understood as a case study of 4 different situations, not future scenarios. In this article, the case studies have been noted as "representative of a decade-RCP", reminding that each future simulation has been chosen among a given decade. As an example, the case study simulated for the meteorological year 2033, under the RCP8.5 tendency, is called 30-RCP8.5.

3.2. Changes in chemical species

Our analysis focuses on a restricted series of compounds, whether primary or secondary, that account for species that are predominantly present in urban and suburban smogs, and aerosol fractions that may be sensitive to climate change and environmental policies. Fig. 6 traces the evolution of the simulated seasonal concentrations of ozone (O_3) and nitrogen oxides (NO_x), but also of particulate matter (PM_{10} and $PM_{2.5}$) and its fractions, for the 4 future case studies, as an average over the

nested domain of our study. Note that whenever a Figure is shown for O_3 in this study, it refers to the simulated daily maxima values (based on 8h running means) in order to be consistent with the regulatory threshold for human health protection. In Fig. 6, the changes in the simulated concentrations between the baseline simulation and each of the scenarios result from both the meteorological specificities of the target year and the associated reduction in anthropogenic emissions. Each panel presents the results of a particular pollutant, with case studies being associated with a given color (2033 simulations in blue, 2053 simulations in red, light colors for RCP4.5 scenarios and dark ones for RCP8.5 scenarios). 2D representations of O_3, NO_x, PM_{10}, $PM_{2.5}$, dust and BSOA concentrations are also presented in Fig. 7. These maps show the mean annual concentrations of the pollutants for the reference simulation (in ppb for ozone, in $\mu g.m^{-3}$ for the PM) and the percentage of deviation from these values, for the scenarios. They allow a spatial discrimination of the evolutions of the pollutant concentrations between the reference and the case study. Note also that, for each species, only the season in which it shows the highest average concentration was displayed, summer for ozone. That is, winter for NO_x, spring for PM_{10}, $PM_{2.5}$ and dust, and summer for BSOA.

The concentrations of primary components such as nitrogen oxides depend directly on their related emissions. Thus, predictably, NO_x concentrations (see Fig. 6-b) show a strong diminution in all scenarios – from -20% to -40% – that is mainly the result of anthropogenic emission control at the horizons 2030 and 2050. The same effect can be observed for the gaseous and particulate ammonium concentrations (ammonium particles - not shown in figure – undergo a decrease ranging from -10% to -50%). On the contrary, a large number of parameters – such as the availability of precursors and atmospheric conditions for chemical transformation – affect the evolution of secondary species such as ozone and BSOA. For ozone, a global decrease is observed, which might be explained by the simultaneous decrease in NO_x and volatile organic compounds (VOCs) emissions, thus leading to reduced

Fig. 6. Seasonal concentration change seen in future scenarios for a number of components (in %). Name of each component is written on the top of the panel. For all future situation, the average changes for all seasons are shown.

photochemical production. However, a strong seasonal dependency is expected for this species, as it can be seen in Fig. 6. In winter, meteorological conditions are unfavorable to the production of ozone, therefore the reduction of ozone titration by NO_x in emitting areas (as seen in Fig. 7) becomes a dominant effect, and leads to the lower average decrease of ozone in Fig. 6. In summer, conditions for ozone production are present, and their concentration gets higher than other seasons (annual average of around 40 ppb). Although titration by NO_x also exists at this season, the main impact of the scenario is the fact that ozone production then becomes strongly unfavorable due to the lower availability of NO_x. As a matter of fact, a maximum reduction of -12% means around 4 ppb of decrease on the average. Spatially, ozone concentrations are higher in the north and north-western parts of the domain, probably because of the more rural nature of these areas (for verification of rural areas please refer to Fig. 4 for population of the region and Fig. 10 for the population density of the domain).

As shown in Fig. 6 (panels c and d), PM_{10} and $PM_{2.5}$ each show decreases as well. This tendency is mostly due to a diminution in the concentrations of nitrates and sulfates (see Fig. 6-e and 6-f) in our simulations. The reason for the decrease of these two species is the respective reduction of NO_x and SO_2 emissions (for a decrease of around -40% and -50% for NOx and -30% and -40% for SO_2 for 2030 and 2050 respectively for France), whereas for nitrates there is an additional effect due to the increase in temperature which leads to a greater evaporation of nitrates already formed (Bauer et al., 2007; Hauglustaine et al., 2014; Seinfeld and Pandis, 2016). No significant change in the salt concentrations is seen in the future case studies, while an increase in dust concentrations is observed in most cases (will be discussed in the next section). Seasonally, their trends in both PM_{10} and $PM_{2.5}$ seem similar: showing smaller changes in winter for both PM_{10} and $PM_{2.5}$ and higher changes in summer and autumn. The changes for spring for PM_{10} seem however to be lesser than and $PM_{2.5}$, probably due to the increase in dust concentrations which are mostly in the coarse size fraction. Spatially, PM_{10} shows high concentrations in the southern and south-western coasts of the domain (Fig. 7), notably because of salt emissions from the sea as well as high sulfate concentrations due to the proximity of industries and maritime traffic. Sulfate concentrations show a similar spatial distribution to total PM, both in reference simulation and future changes, higher concentrations in southern coastal areas and a future decrease for all seasons. Nitrates though, show higher concentrations in northern part of the domain, though the spatial variation of the future changes stay quite homogeneous all throughout the domain. The transport of dust particles is another reason for the higher concentrations of PM_{10} near the Mediterranean coasts, this transport has been shown in different studies such as Israelevich et al. (2012); Denjean et al. (2016); Vincent et al. (2016). Its concentration as an average shows a diminution in all test cases (lowest change for 30-RCP8.5), while showing a stronger signal near the coast lines. $PM_{2.5}$ shows a similar spatial distribution to PM_{10}, its changes in future case studies showing a more homogeneous decrease across the domain.

Unlike other major particle fractions, BSOA mass concentrations increase in the majority of our future case studies (Fig. 6-h). This change is attributable to the increase in temperature in the scenarios; because of that, biogenic VOCs (BVOCs) emissions are simulated to step up, resulting in greater production of secondary organic aerosol (Cholakian et al., 2019a). However, opposite effects have to be considered for BSOA. Indeed, higher temperatures may thermodynamically limit the transfer of gaseous semi-volatile VOC (SVOC) to the particulate phase (Cholakian et al., 2019b). Another process that impacts the BSOA budget is the CO_2 inhibition added to MEGAN in this work, where with higher CO_2 concentrations come lower isoprene emissions. In our simulations, the increase of the BSOA particulate mass is the dominant effect in RCP8.5 scenarios (dark colors), while a slight global decrease is simulated in the RCP4.5 scenarios (light colors) for most of the seasons. It therefore seems that the increase of BVOC emissions in the hottest scenarios eclipses the effects of BVOC phase equilibrium, and that the impact of CO_2 on
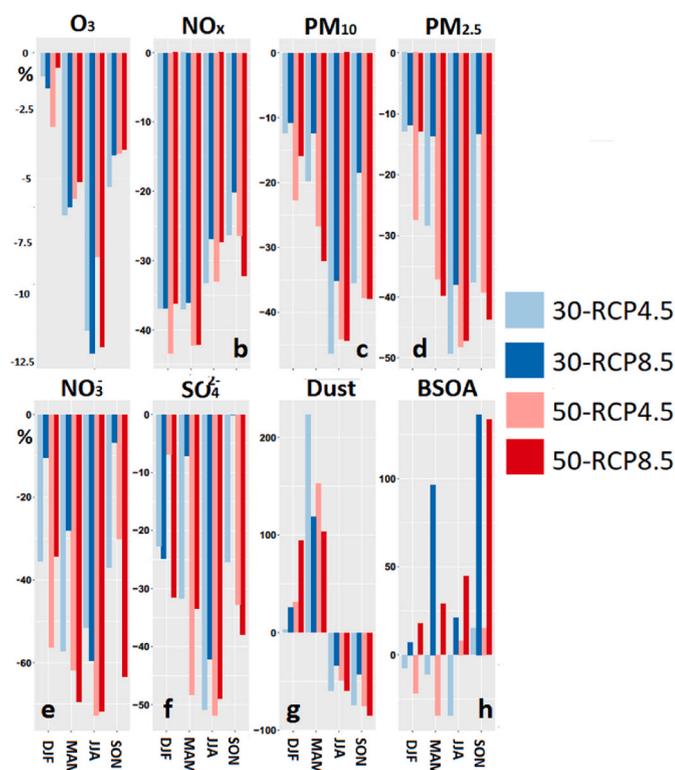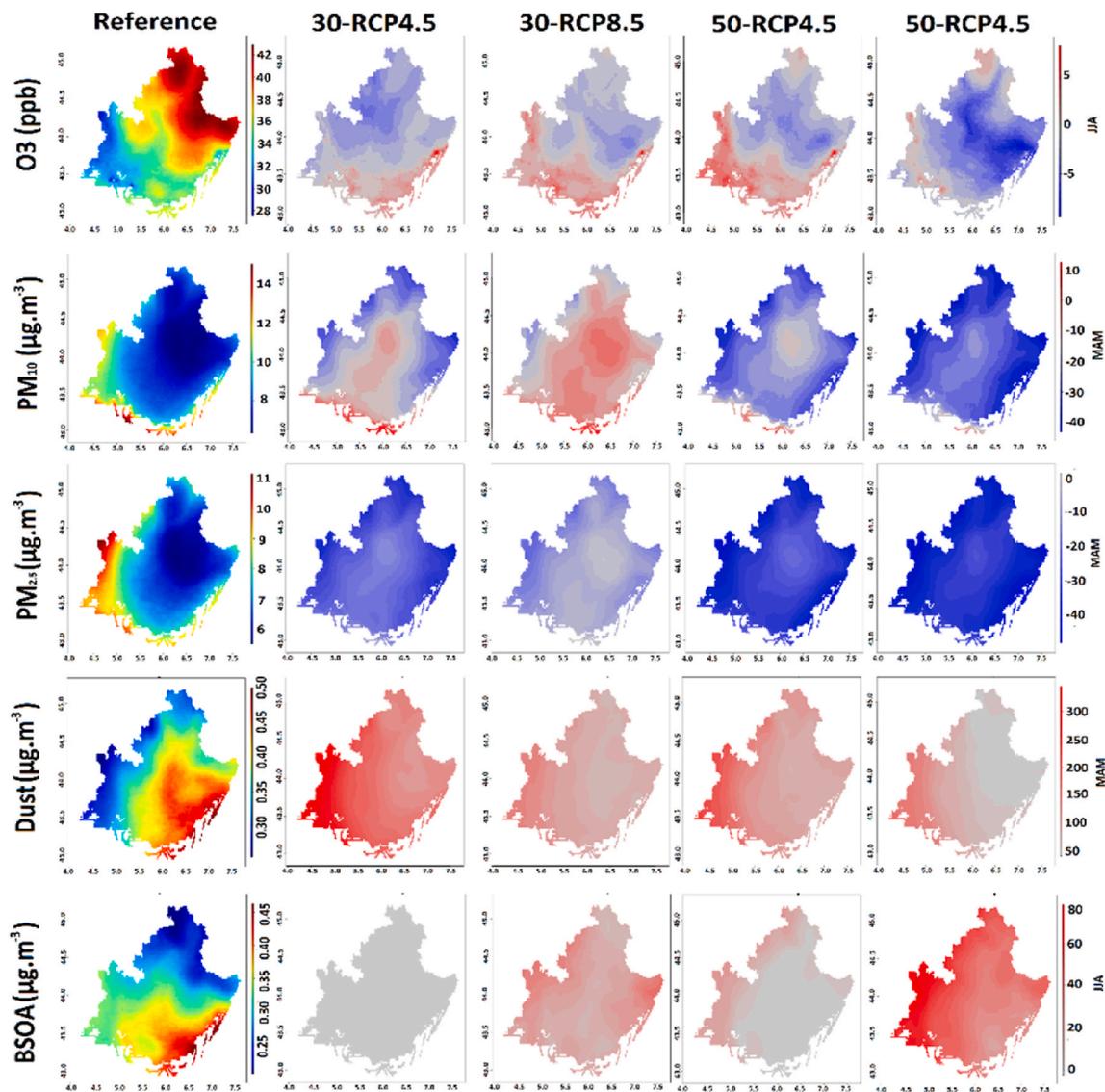
Fig. 7. 2D representations of ozone, PM10, PM2.5, dust and BSOA concentrations for the PACA region. The first column on the left shows the absolute annual concentrations in the historic simulation (2005), while the four right columns show the change in concentrations relative to the historic simulation for each RCP case study. Each row shows one species, for the season in which the concentration shows the highest changes. The name of each scenario is written above each column and the name of each component is written on each row.

isoprene emissions is then of the second order. Quantitatively, the increase in BSOA concentrations become quite high in 50-RCP8.5 (dark red bars), reaching a factor of 2 in spring and exceeding it in fall. It is important to take into account that changes in soil humidity have not been taken into account in the BVOC emission changes.

It seems to be a logical possibility that dust emissions could increase in future scenarios: droughts, land use changes and deforestation will result in broadened dust emissions, all three of which being probable outcomes in future scenarios (Brey et al., 2020); although the uncertainties concerning this species in future scenarios is so high that it is hard to say for certain how its emissions will be affected (Tegen et al., 2004; Evan et al., 2014). As for this study, dust concentrations double in spring in all scenarios (see Fig. 6-g), while they strongly decrease in summer and fall. Spring is the period when the most significant dust episodes take place in the northern African deserts, the dust-rich air masses being transported partly to the Mediterranean, thus affecting the PACA region (Vincent et al., 2016). Dust concentrations are high at the southern coasts of the domain, because of their transport from Northern coasts of Africa towards the south-western coasts of the PACA region. They show an increase in concentration in all case studies, for this area,

and especially in spring. This being said, there are major uncertainties when it comes to the simulation of dust concentrations, especially regarding to how they have been taken into account in the global model which has been used as boundary conditions.

Changes in the concentration of the gaseous and particulate species analyzed here, combined with future population projections, result in variations in the exposure of the population to each of these species. Total and spatialized population exposure, in the different scenarios, are explored in the following section.

3.3. Population exposure to atmospheric components in future scenarios

We combined the population density maps and the concentration fields of the main pollutants simulated with CHIMERE, in the current situation and for the years 2033 and 2053, for the RCP4.5 and RCP8.5 scenarios, for each of the different demographic scenarios. As mentioned above, the presentation of the results will be based on the SSP3 and SPP5 projections only.

We first conducted a seasonal analysis of the evolution of exposure from the historic run, and the results are only presented for the least

favorable seasonal situations of each SSP. These data are presented in the form of 2D fields, for each pollutant and demographic/climatic scenario, in order to identify spatial disparities in the evolution of the "exposure" parameter. Finally, in order to address the issue of dense inhabited regions versus rural areas, we have searched for the areas where the model would predict a greater sensitivity to the climatic scenarios and the selected years. To this end, we present plots for each county, an administrative division which allows to distinguish 6 zones in the PACA region. All these results allowed us to define trends in the evolution of the exposure of the population in the PACA region between the current situation and warm future years, and to determine in which situations, in which zone and for which pollutants and seasons the evolution of the exposure was the most unfavorable of all case studies.

3.4. Exposure analysis for the entire PACA region

Fig. 8 shows the results of exposure calculations for the 6 studied species and seasons presented in previous figures, for each climatic scenario and for the SSP3 and SSP5 demographic projections. The values shown in the panels correspond to the percentage of change in total exposure (second and third rows of charts), compared to the baseline

population exposure (first row). Each color corresponds to one of the 4 future situations studied: 30-RCP4.5 and 30-RCP8.5 (light and dark blue) and 50-RCP4.5 and 50-RCP8.5 (light and dark red).

On the average, total exposure shows a strong reduction for background nitrogen oxides and for particulate matter in both size fractions. This decrease ranges from −53% to −63% for nitrogen oxides and from −5% to −50% (depending on the case study, season and fraction) for particulate matter, in the selected SSP scenarios. It can be concluded that the reduction of emissions is never offset by the increase in the population, since the total health risk decreases whatever the season and the case study simulated with CHIMERE. Of the 4 simulated future situations, we can see in both figures that the effect on NO_x exposure is very little sensitive to the season and to the considered time frame, and that the difference between the two population scenarios is moderate, showing smaller decrease in exposure when the more densely populated SSP is discussed. It is interesting to note that exposure reduction is quite strong for this species since the NO_x are primary pollutants and future emissions reductions should have a significant impact on their concentrations.

Exposure to ozone appears highly dependent both on the demographic scenario and the time horizon at which the analysis is
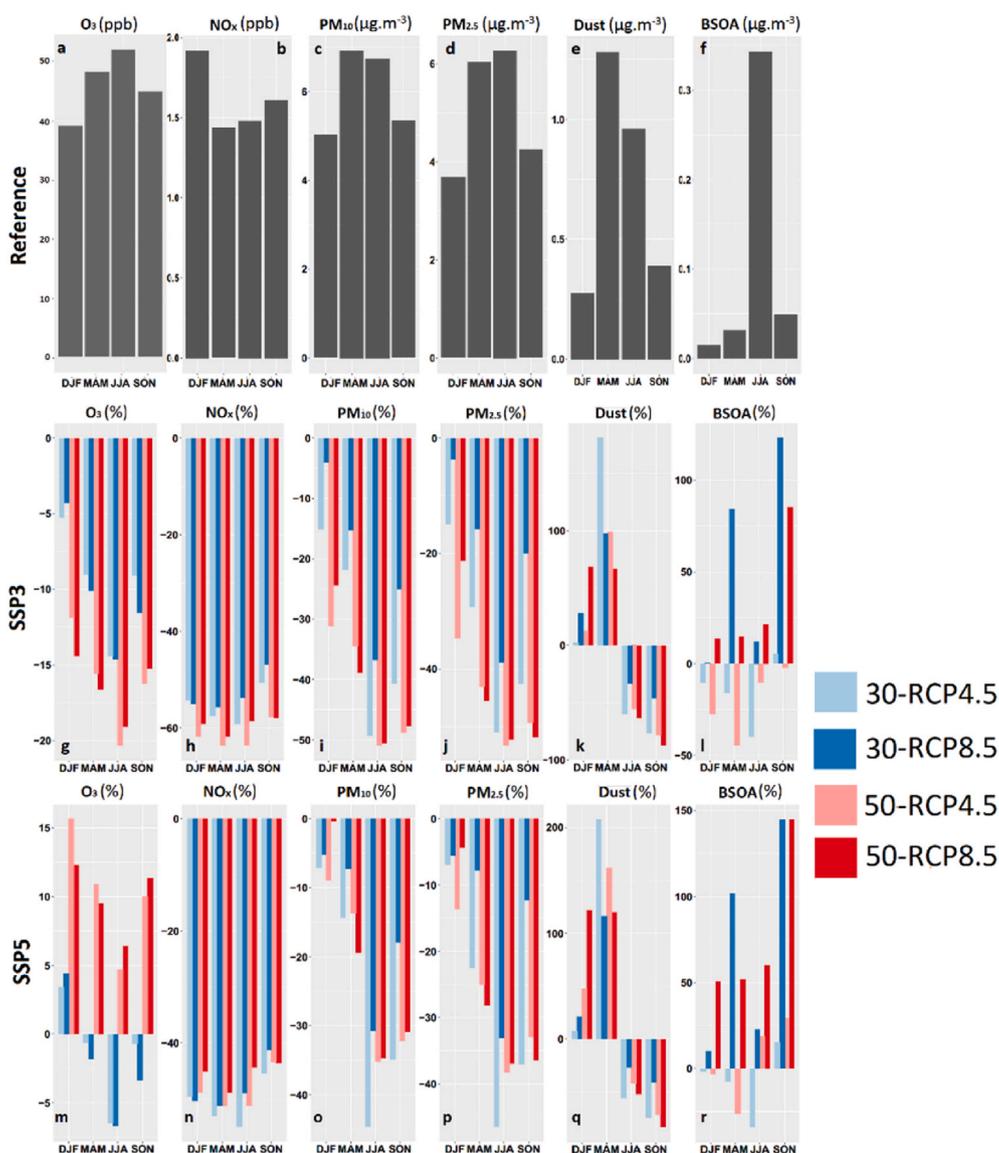

Fig. 8. Population-weighted exposure in the reference simulation and its changes (in %) compared with the reference simulation for the SSP3 and SSP5 demographic scenarios, presented by season and for ozone, nitrogen oxides, particulate matter, dust and BSOA. The name of the species is shown above each panel.

conducted. In the SSP3 (Fig. 8-g) scenario where the population increase is moderate (in particular for urban areas), the general trend is a decrease in total exposure to ozone for all the modeled situations (around −10% on average). The 50-RCP4.5 and 50-RCP8.5 simulations are the most favorable, mostly because they show a decrease in the total population in the region. For SSP5 simulations, on the reverse, CHIMERE predicts a moderate increase in total ozone exposure in the most distant scenarios (from 5 to 15%) and for the whole year, whereas for the 2030 horizon this effect is close to 0 (less than 5% of variation). Interestingly, exposure is always 10–15% lower in 2030 than in 2050, while it is similar for the RCP4.5 and 8.5 pathways.

For both the SSP5 and SSP3 scenarios, we also note that the evolution of exposure is always more favorable in summer (owing to the decrease in the ozone maxima) than in winter (when the reduction of titration by NO is dominant). Largest differences between SSP3 and SSP5 occur in the 2050 scenarios. Reasons for this will be given in the next section.

On the other hand, the signal observed on the particles is much more variable. Two major effects are observed in our case studies. Firstly, the expected decrease in total PM exposure is greater in summer and fall and lower in spring, especially for PM_{10}. This is at least partly an effect of the increased dust particles concentrations in spring. Second, for both PM size fractions, in the short term (2030, blue bars), there is a very high sensitivity of total exposure to the RCP scenario, with a much less favorable situation for the hot 30-RCP8.5 situation (dark blue bars) for both demographic projections. This suggests that climatic conditions play a very important role in particle exposure, in a scenario in which emission inventory is little different from that of today. This is no longer the case in the 2050 simulations, when both RCP scenarios are very favorable, suggesting that the prevailing effect is the long-term reduction of particulate emissions.

It is important to mention that the sensitivity to the demographic scenario is significantly higher for PM_{10} than for $PM_{2.5}$. We have seen in Fig. 7 that the concentration variation in PM_{10} was strongly localized on the Mediterranean coast, a rather highly urbanized area. We can therefore conclude that the demographic scenario (and in particular the increase in the coastal population) is a driving element for PM_{10} exposure in our PACA simulations, in addition to dust concentrations (see below). Since this is highly dependent on the dust fraction, for which the contribution increases in spring (Fig. 8-k and 8-q), it will be interesting to analyze in detail the spatialization of the risk of dust exposure in the different SSP scenarios (see below). Albeit they make up an important part of the PM10 concentration, we didn't consider the role of sea salts in this analysis, as their concentrations were very little variable from one situation to another (as also mentioned before). Conversely, sensitivity to the SSP scenario is lower for $PM_{2.5}$ than PM_{10} in our 4 future situations. Part of this effect is due to the fact that the different components of this fraction (BSOA, nitrates, sulfates) follow very different behaviors in our scenarios. In fact, despite decreasing exposure to nitrate and sulfate fractions, we note that CHIMERE predicts a significant increase in the concentration of the biogenic SOA particulate fraction in the case studies associated with the strongest temperature increases (30-RCP8.5 and 50-RCP8.5). This result generally leads to an increase in total exposure to BSOA in the PACA region, even if the amplitude of the effect is extremely dependent on the climatic conditions. Another reason for the low dependence of $PM_{2.5}$ exposure on the SSP scenario is the fact that some of the $PM_{2.5}$ components are secondary fractions whose formation is strongly climate dependent (BSOA notably). This analysis will be completed in the following section with a 2D-plot of the risk of exposure to $PM_{2.5}$.

3.5. Spatial analysis of the simulated exposure tendencies

As an averaged value does not fully capture changes in population exposure, we conducted a spatial analysis of the results. In Fig. 9 are reported only the species presenting marked spatial tendencies, for the SSP5 scenario.

The 2D maps presented in Fig. 9 represent the evolution of exposure between the historical simulation and each of the future case studies for the SSP5 demographic scenario. In the case of ozone, this Figure shows that urban areas – mainly located on the coast - are subject to increased total exposure, combining both increased concentrations (increased individual exposure) and population growth (increased total risk). These maps are congruent with population growth (Fig. 4-c to 4-f), indicating that population growth is once again the driving parameter of total exposure in our study. However, red areas extend beyond the boundaries of dense urban centers (see the land use map in Fig. 4-b). This indicates that exacerbated ozone exposure also affects the sub-urban areas of the region. Conversely, inland, in the most rural areas, there is a downward overall risk of exposure to ozone, for all the future situations considered in this work. On the average, increased exposures over the coastal areas dominate in absolute terms, which leads to the largest summertime ozone exposure increases for the 2050 SSP scenario.

Spatial patterns are particularly visible for the dust component of PM_{10}. Indeed, there is an increased exposure of at least 40% on all urban grid points (see urban land use in Fig. 4-b). When we cross this map with Fig. 7, which shows that the increase in dust concentrations affects especially the South and West of the domain, we can conclude that – for our scenarios – there is an increased individual (due to concentration rise) and total (due to increased population) risk of exposure to dust on the French Mediterranean coast. We have referred above to the issue of dust as potential vectors of microorganisms such as viruses. In this context, the facilitation of dust transport by favorable climatic conditions (wind, drought) must be considered as a health risk factor for populations over the western Mediterranean basin. However, to better assess the evolution of dust particle sources in future situations, it is necessary to work on the evolution of land use in African source areas. In other words, the land use changes that will occur because of climate change should be considered in order to change the emissions of dust that arrives to the studied domain here (either via changing the land use itself or via changing the boundary conditions used in future test cases), otherwise only the meteorological effects of climate change will be visible on the concentration of dust in the tested future situations.

The same spatial analysis can be conducted for the evolution of the BSOA fraction of PM2.5 particles, as the largest increase in the total exposure risk is observed in areas experiencing the strongest population increase. However, the comparison of case studies that differ greatly in the mean annual temperature (in particular 30-RCP4.5 and 30-RCP8.5) shows that the evolution of exposure to the BSOA fraction remains mainly dependent on climatic conditions.

3.6. Localization of the main risks

As explained above, high spatial variability is seen in the exposure of the population with urban areas showing higher total exposure than rural areas. Also, current air pollution related mortality studies show that the PACA region in general presents high rates of mortality, with very strong relationships between the evolution of respiratory and cardiovascular diseases and that of urban concentrations of pollutants (Sicard et al., 2010, 2011). In order to support health risk management, it is essential to identify the typologies of areas that are most involved in global risk, as well as those where this overall risk evolves most over time.

This is why we propose a first approach to risk management support by looking at the geographical distribution of the risk of exposure, taking into account territorial divisions. We have divided the PACA region into its administrative counties, corresponding to the French sub-regional "*departements*" in France. Our first goal is to determine whether all the geographical zones of the domain show similar total risks related to air pollutant exposure, or if it appears specific zones carrying a greater part of the total risk, or even areas particularly sensitive to future climate and socio-demographic trends, such as those simulated in our case studies.

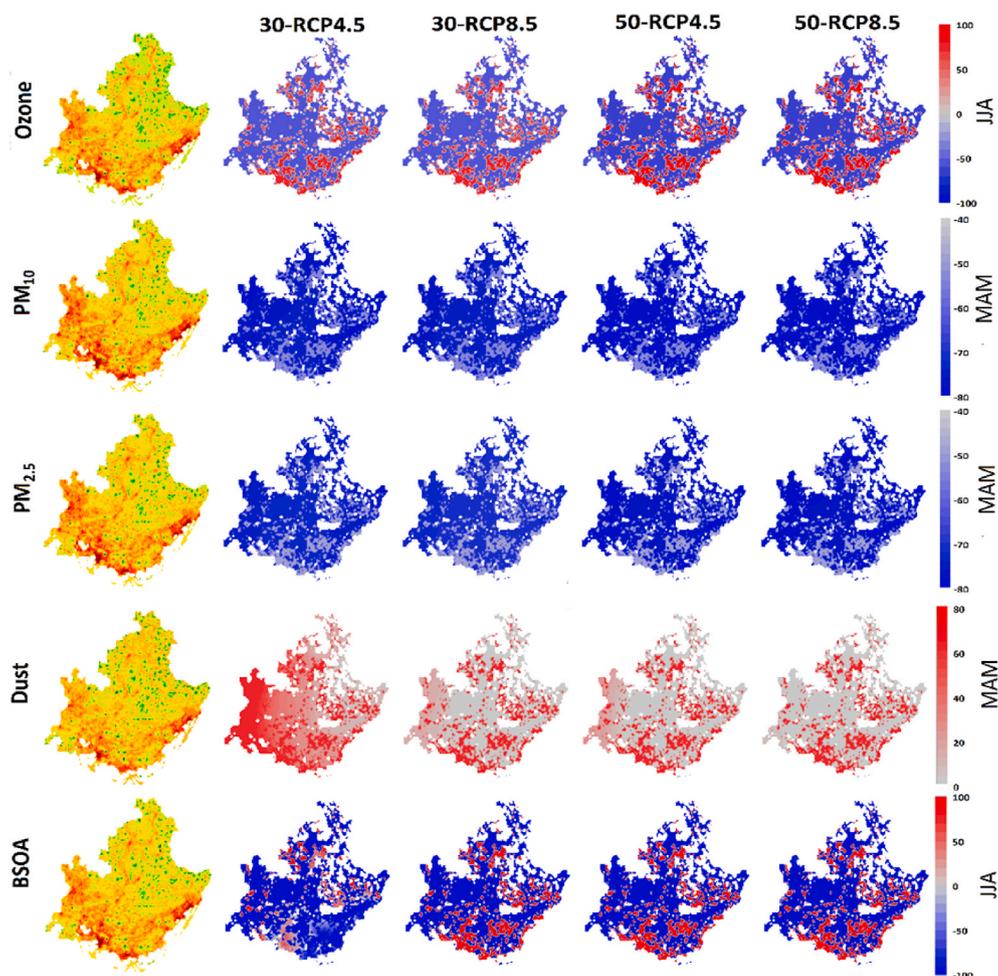For these purposes, we used the works of Yao et al. (2014) who

Fig. 9. 2D representations of exposure to ozone, PM10, PM2.5, dust and BSOA for the PACA region for the SSP5 scenario. The first column on the left shows the exposure in the historic simulation (2005), while the four right columns show the changes relative to the historic simulation for each RCP scenario. Each row shows one species, for the season in which the exposure shows the most dramatic changes. The name of each scenario is written above each column and the name of each component is written on each row.
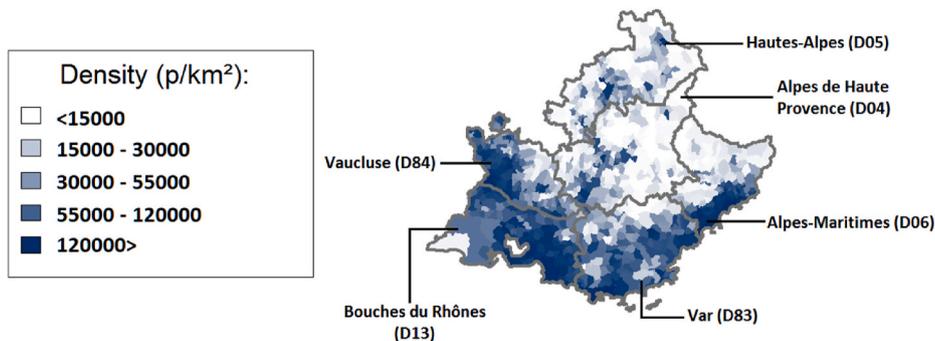

Fig. 10. Counties of the PACA region and associated population density. The region regroupes six counties: D06, D13, D83 and D84 -> dense and urbanized and D04, D05 -> predominantly rural.

developed an exposure index for particulate matter based on a population-weighting calculation (called the WEI index). This index allows us to (take into account the population distribution and) propose a spatialized quantitative assessment of the risk associated with exposure to pollution. It is obtained from the following equation:

$$\text{Weighted exposure} = \sum_{i=1}^{n}\left(C_i \times \frac{P_i}{\sum_{i=1}^{n}P_i}\right)$$

Where.

C_i Concentration in cell i

P_i Population of cell i

$\sum_{i=1}^{n}P_i$ Sum of population in all cells

All the values shown in this section have been calculated using this equation.

3.7. County per county analysis

The six administrative departments of the PACA region are presented in Fig. 10. All have strong gradients of population density, but four of them show an important share of dense urbanized areas (D06, D13, D83

and D84) while the other two (D04, D05) are predominantly rural. In particular, the three counties including a Mediterranean side (Bouches du Rhônes (13), Var (83) and Alpes Maritimes (06)) have a very high density of population because they shelter the large urban areas of Marseille, Toulon and Nice respectively. Taken together, these cities account for about 30% of the total population of the region.

For each of the 6 counties in PACA, we calculated the Weighted Exposure Indicator (WEI) and applied it to all the previously discussed atmospheric components. For a given pollutant in a given department, the calculation consists in multiplying the population of each cell in the sub-domain by the average concentration simulated in this cell, and then divide the result by the total population of said department, all the values obtained for d being finally summed up. Such a process provides the weighted exposure index of the population for this department. The results for this analysis are shown in Fig. 11 (for SSP3) and Fig. 12 (for SSP5). For each component, the weighted exposure calculated for each county in the reference case study is shown in the first column, while the absolute differences between the future situations and the historic simulation have been plotted in the second to fifth columns. For each component, only the season showing the largest changes is shown (written on the side of each line).

In the reference case, the WEI of ozone is high for all coastal counties, which can be explained by their large population, but it is noted that the northern rural county also has a fairly high value, highlighting the accumulation of ozone along the path of the air mass in the region. When exploring the future case studies, a dual behavior is seen for the ozone WEI in SSP3 (decreases everywhere) and SSP5 (increases everywhere). The WEI changes for ozone are dependent on multiple factors: (i) emission reductions, therefore showing a higher change in exposure in the 2050 timeframe simulations when greater emission reductions are achieved, (ii) population increase, therefore showing heightening exposure in SSP5 and lowering exposure in SSP3, (iii) land-use dependency: counties that are home to major cities showing lower exposure reduction in the case of SSP3 and higher exposure increase in the case of SSP5 due to reduced titration and finally (iv) climate change related effects (higher temperature for example). The evolution of the ozone WEI in SSP5 is particularly contrasted between the different counties, since the 3 coastal departments show increases of the index which are up to 4 times stronger than in the rural ones. This increase is not negligible compared to the gap that currently exists between the departments, and it shows that the risk associated with ozone in urban areas must be taken into consideration.
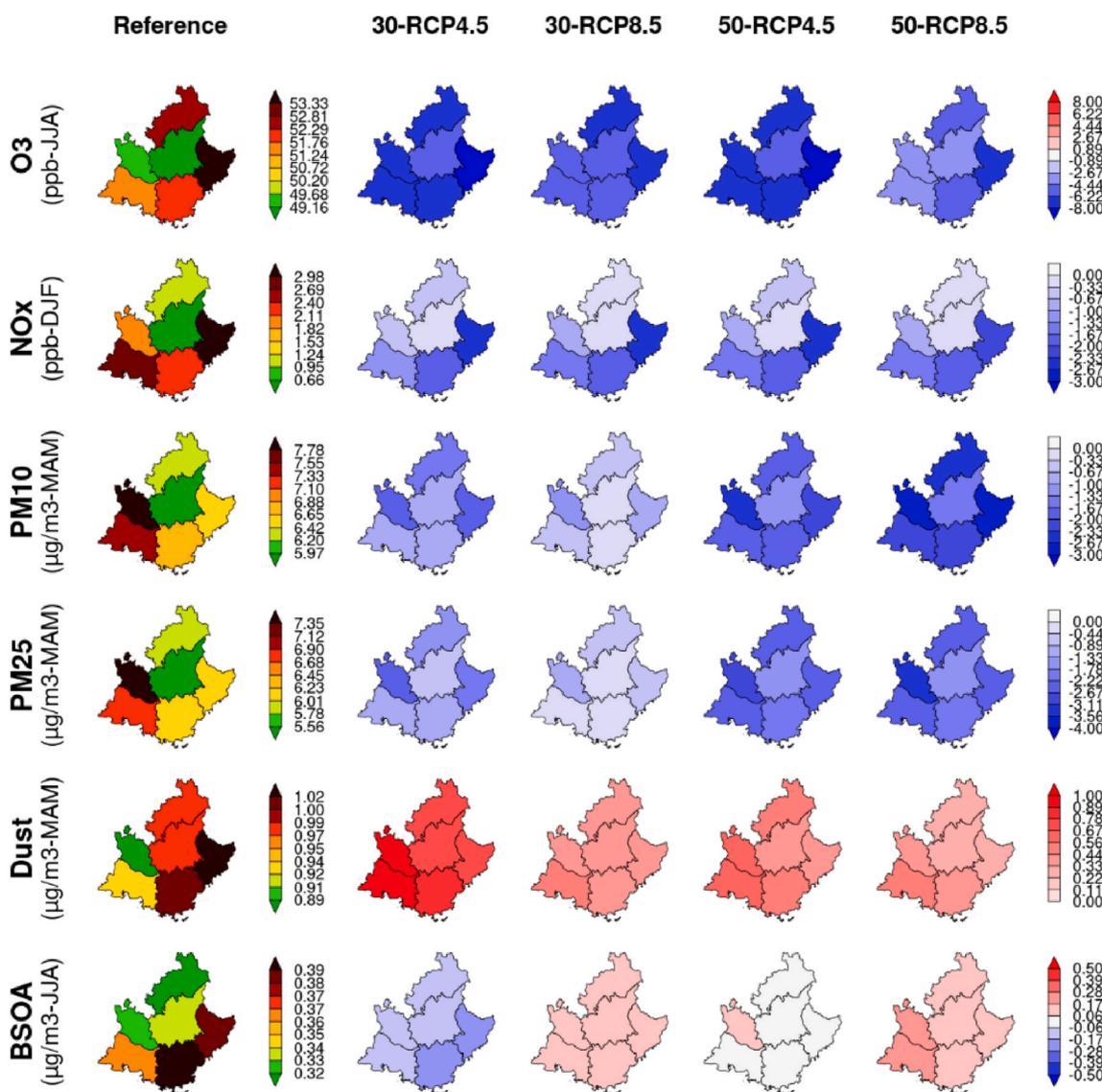

Fig. 11. Population-weighted exposure in different departments for the SSP5 scenario. The historic values are shown in the top panels. The changes between future and historic case studies are shown on the second to fifth columns. The units and the plotted season are written at the left of each row.
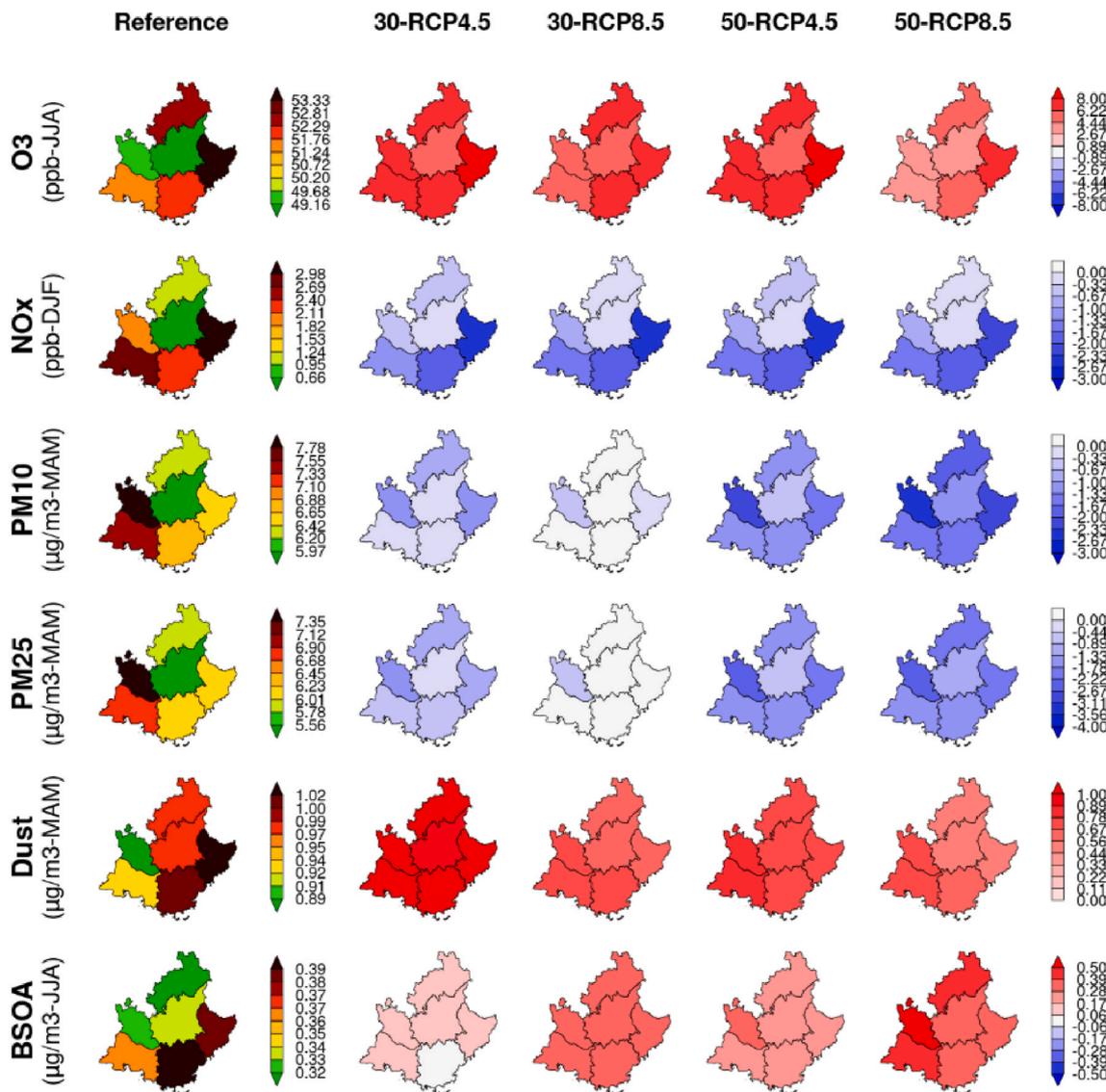
Fig. 12. Population-weighted exposure in different departments for the SSP5 scenario. The historic values are shown in the top panels. The changes between future and historic case studies are shown on the second to fifth columns. The units and the plotted season are written at the left of each row.

As can be seen in Fig. 11, nitrogen oxides show a higher total exposure risk in the coastal, urbanized and industrialized counties (D13, D84 and D06), the exposure for D06 being more than four times that of D04. When exploring the changes in the exposure, the urban and industrial counties show the largest changes, both in SSP3 and SSP5 demographic scenarios, because they house almost all the anthropogenic emissions related to transport, industrial and shipping activities (Figs. 11 and 12) of the region. In the end, the scenarios tend to show a reduction of inequalities between urban and rural departments, since the excess of risk on the current situation in departments D06 and D13 are same order of magnitude as expected gains (up to 2 μg m^{-3}).

Both PM$_{10}$ and PM$_{2.5}$ show higher WEI in D84 and D13, followed by D83 and D06, the 2 remaining counties showing low WEI indexes in the reference simulation. In the future simulations, exposition to both PM size fractions decreases in all subdomains. It is important to note the role of the demographic scenario in the final outcome, since the exposure in SSP5 decreases less (from a factor of 0.75 to a factor of 0.25) than in SSP3 due to a higher expected population growth. In all the simulated scenarios, D84 shows the highest reduction in PM exposure, followed by D05 and D06.

Similarly, to PM, dust particle exposure is rather heterogeneously

distributed all around the region, but significantly higher exposure being calculated for western counties (D83 and D06 showing the highest and D13 and D84 showing the lowest exposure) in our baseline simulation. In all our future case studies, dust particles are associated with an increasing exposure level in all counties and quite uniformly across the domain, while showing higher increase in SSP5 rather than SSP3. However, according to CHIMERE, the western fringe of the domain is particularly exposed to dust intrusions, which - together with the increase in population - leads to a greater increase in the weight of the 3 western departments in the total exposure, and calls for greater vigilance on the issue of dusts, as vectors of other contaminants on these regions (Figs. 11 and 12). This is particularly visible for scenario 30-RCP4.5 in SSP3, characterized by large wind speed, while in SSP5 the effect of the increasing population becomes more prevalent. As the order of magnitude of the expected changes is greater than the differences between counties, our results indicate that climate and demographic evolutions are likely to modify very strongly the relative weight of the departments in the total exposure to dust.

As far as BSOA is concerned, it can be seen that the D06, D13 and D83 coastal departments group the highest shares of current exposure, due to the proximity between inhabited urban areas and sub-urban areas where

BSOA-type aerosols can be formed (Figs. 11 and 12). D05 is a remote mountainous area with low population and local pollution conditions do not favor BSOA production, which explains why it shows the lowest exposure for this species. There seems to be a south-north gradient for the BSOA exposure (decreasing towards the north) which corresponds both to the population density and also the predominant anticyclonic condition favorable for the AOS formation. Almost all counties respond in the same way to future case studies, with an increase in the total exposure risk for the 2 hottest situations (30-RCP4.5 and 50-RCP8.5) in SSP3, and an increase in risk in all situations for SSP5 (Figs. 11 and 12). Similarly, to dust, the expected changes can strongly change the relative share of the different counties in exposure. We note that each time, whatever the demographic scenarios, it is the D13 and D84 departments that are most likely to see their total risk worsen.

This territorial analysis shows us that - in our case studies - the evolution of exposure to our target atmospheric pollutants is (in most cases) critical in coastal areas, but this spatial tendency is not the same for all pollutants. In particular dust and BSOA particles show specific evolution depending on the location of their sources, and long-distance transport. These differences underline the importance of spatialized management of health issues.

4. Summary and conclusions

The focus of this article is the exposure of the population in PACA, a densely populated area located in the south-east of France and adjacent to Mediterranean Sea, with respect to future case studies of atmospheric pollutant evolution. For this purpose, five years of simulations were performed, one for the historic simulations and four future case studies chosen from the 2030 and the 2050 decades under RCP4.5 and RCP8.5 climate change trajectories. For each simulation, anthropogenic emissions for the corresponding year have been prepared using the current legislation (CLE) emission scenarios. In order to explore the exposure changes of the population, the current and the future population is needed for the aforementioned region.

The simulations show a decreasing concentration of O_3, NO_x, PM_{10} and $PM_{2.5}$ because of anthropogenic emission reductions of nitrogen oxides, VOC and SO_2. At the same time, an increase in BSOA and dust concentrations is seen in most of the future situations examined in this study, for summer and spring period respectively. The increase in BSOA and dust particles is compensated by the decrease in nitrates and sulfates, resulting in a diminution of total PM_{10} and $PM_{2.5}$ concentrations. Of course, each of these components shows a specific seasonal and spatial behavior. Seasonally, the concentrations of PM_{10}, $PM_{2.5}$ and dust are maximum in spring, while for BSOA this maximum is achieved in summer. In this article, seasons with maximum concentration for each species are explored.

The exposure of the population was analyzed for the species mentioned above, for both historic and future case studies. Spatially, the exposure is maximum in areas where the population density is more important, meaning urban areas. Albeit the increase of the urban population in all future population scenarios, a decrease is seen in population exposure because of the reduction in the concentrations of the pollutants mentioned above. An exception is seen for dust aerosols, where the exposure of the population to this particulate fraction grows in all future situations studied. A decreasing population exposure to PM_{10} and $PM_{2.5}$ pollution means that the effects of this pollutant on the human health can be reduced in the future, albeit increasing populations.

While this is true for PM_{10} and $PM_{2.5}$, the exposure to dust and BSOA fractions becomes higher in spring and summer, respectively, in the future scenarios explored in this work. This is a significant result, since dust particles are one of the species likely to increase exponentially in the future due to land use changes, deforestation and droughts related to climate change. Therefore, an increasing exposure to dust particles can increase the risk of common diseases caused by atmospheric particulate matter as well as the possibility of bacterial, fungal and viral diseases. In addition, the formation of BSOA particles have a high dependence to temperature, which is expected to increase in the future.

Finally, exposure in the administrative counties in the PACA region is analyzed in this work, using a population weighted approach. The PACA contains 6 counties, three of them being highly populated with major urban areas. The exposure to ozone shows a growing trend in these counties (D13, D83 and D06), while diminishing in the other ones (D04, D05 and D84). Exposure to dust and BSOA particles is increasing throughout the region, but the trend is also, to some extent, determined by the population of the urban counties. This means special attention should be given to urbanization and urban area growth since it can result in more exposure to certain atmospheric pollutants for a higher population density.

Our results show that the engaged emission reduction policies may be effective in reducing the total exposure of the PACA region's population to air pollution. This will make it possible to combat primary air pollutants or those formed near the emitting zones, such as nitrogen oxides, sulfates, nitrates and more generally, most of the PM mass. However, this is not true for all atmospheric pollutants. Long-range transport can affect the exposure of the population in this region as well, for example through the transport of dust particles from Northern Africa. Temperature-dependency of the production of species such as BSOA can affect the exposure of the population as well, with an increase in this exposure as the temperature rises. These last two particulate fractions cannot be controlled by local emission reduction policies and a more comprehensive policy is needed to mitigate this exposure.

A future step in this work would be to explore land use changes in this region and include hypotheses on the increase in dust emissions from North Africa, which would lead to changes in dust concentration in the PACA region. Also, boundary/initial condition forcings should be taken into account and studied in more detail specially when it comes to dust emission and transport schemes. Another point would be to explore the exposure based on different age groups and then calculate the mortality for these age groups because of concentration changes in future scenarios. Furthermore, it would be worth doing a similar study on other parts of the Mediterranean area in order to see if the same hypothesis can be made for different types of profiles: dense coasts, rural areas, hotter areas, etc. Finally, it would be interesting to repeat the same experience with longer simulated periods, therefore passing from case studies to future scenario assessment.

CRediT authorship contribution statement

Arineh Cholakian: Conceptualization, Methodology, performing and analyzing the simulations and writing. **Isabelle Coll:** Conceptualization, Methodology, Supervision. **Augustin Colette:** Supervision. **Matthias Beekmann:** Supervision.

Declaration of competing interest

Acknowledgements

Cordex simulations, and Didier Hauglustaine and Sophie Szopa are acknowledged for providing the INCA simulations. Zbigniew Klimont is acknowledged for providing ECLIPSE-v4 emission projections. INERIS and LCSQA are acknowledged for providing population data for the PACA region. AtmoSud is acknowledged for providing the high-resolution anthropogenic emission data for the PACA region. The thesis work of Arineh Cholakian is supported by ADEME, INERIS (with the support of the French Ministry in charge of Ecology), and via the ANR SAF-MED project.

References

Adloff, F., Somot, S., Sevault, F., Jordà, G., Aznar, R., Déqué, M., Herrmann, M., Marcos, M., Dubois, C., Padorno, E., Alvarez-Fanjul, E., Gomis, D., 2015. Mediterranean Sea response to climate change in an ensemble of twenty first century scenarios. Clim. Dynam. 45 (9–10), 2775–2802. https://doi.org/10.1007/s00382-015-2507-3.

Alfaro, S.C., Gomes, L., 2001. Modeling mineral aerosol production by wind erosion: emission intensities and aerosol size distributions in source areas. J. Geophys. Res. Atmos. 106 (D16), 18075–18084. https://doi.org/10.1029/2000JD900339.

Alfaro, S.C., Gaudichet, A., Gomes, L., Maih, M., 1998. Mineral aerosol production by wind erosion: aerosol particle sizes and binding energies. Geophys. Res. Lett. 25 (1), 991–994. https://doi.org/10.1029/98GL00502.

Amann, M., Klimont, Z., Wagner, F., 2013. Regional and global emissions of air pollutants: recent trends and future scenarios. Annu. Rev. Environ. Resour. 38 (1), 31–55. https://doi.org/10.1146/annurev-environ-052912-173303.

Anderson, J.O., Thundiyil, J.G., Stolbach, A., 2012. Clearing the air: a review of the effects of particulate matter air pollution on human health. J. Med. Toxicol. 8 (2), 166–175. https://doi.org/10.1007/s13181-011-0203-1.

Bank World, 2017. World income classification. Available from: http://www.piscomed.com/wp-content/uploads/2017/03/Income-classification.pdf. (Accessed 26 September 2018). Accessed.

Bauer, S.E., Koch, D., Unger, N., Metzger, S.M., Shindell, D.T., Streets, D.G., 2007. Nitrate aerosols today and in 2030: a global simulation including aerosols and tropospheric ozone. Atmos. Chem. Phys. 7 (19), 5043–5059.

Brey, S.J., Pierce, J.R., Barnes, E.A., Fischer, Emily V., 2020. Estimating the spread in future fine dust concentrations in the Southwest United States. J. Geophys. Res.: Atmosphere 125.

Cholakian, A., Beekmann, M., Colette, A., Coll, I., Siour, G., Sciare, J., Marchand, N., Couvidat, F., Pey, J., Gros, V., Sauvage, S., Michoud, V., Sellegri, K., Colomb, A., Sartelet, K., Langley DeWitt, H., Elser, M., Prévot, A.S.H., Szidat, S., Dulac, F., 2018. Simulation of fine organic aerosols in the western Mediterranean area during the ChArMEx 2013 summer campaign. Atmos. Chem. Phys. 18 (10), 7287–7312. https://doi.org/10.5194/acp-18-7287-2018.

Cholakian, A., Colette, A., Coll, I., Ciarelli, G., Beekmann, M., 2019a. Future climatic drivers and their effect on PM10 components in Europe and the Mediterranean Sea. Atmos. Chem. Phys. 19, 4459–4484. https://doi.org/10.5194/acp-19-4459-2019.

Cholakian, A., Beekmann, M., Coll, I., Ciarelli, G., Colette, A., 2019b. Sensitivity of organic aerosol simulation scheme on biogenic organic aerosol concentrations in climate projections. Atmos. Chem. Phys. 13209–13226. https://doi.org/10.5194/acp-19-13209-2019.

Ciardini, V., Contessa, G.M., Falsaperla, R., Gómez-Amo, J.L., Meloni, D., Monteleone, F., Pace, G., Piacentino, S., Sferlazzo, D., di Sarra, A., 2016. Global and Mediterranean climate change: a short summary. Ann. Ist. Super Sanita 52 (3), 325–337. https://doi.org/10.4415/ANN_16_03_04.

Colette, A., Andersson, C., Baklanov, A., Bessagnet, B., Brandt, J., Christensen, J.H., Doherty, R., Engardt, M., Geels, C., Giannakopoulos, C., Hedegaard, G.B., Katragkou, E., Langner, J., Lei, H., Manders, A., Melas, D., Meleux, F., Rouïl, L., Sofiev, M., Soares, J., Stevenson, D., Tombrou-Tzella, M., Varotsos, K.V., Young, P., 2015. Is the ozone climate penalty robust in Europe? Environ. Res. Lett. 10 (8), 084015 https://doi.org/10.1088/1748-9326/10/8/084015.

Coll, I., Lasry, F., Fayet, S., Armengaud, A., Vautard, R., 2009. Simulation and evaluation of 2010 emission control scenarios in a Mediterranean area. Atmos. Environ. 43, 4194–4204. https://doi.org/10.1016/j.atmosenv.2009.05.034.

Denjean, C., Cassola, F., Mazzino, A., Triquet, S., Chevaillier, S., Grand, N., Bourrianne, T., Momboisse, G., Sellegri, K., Schwarzenbock, A., Freney, E., Mallet, M., Formenti, P., 2016. Size distribution and optical properties of mineral dust aerosols transported in the western Mediterranean. Atmos. Chem. Phys. 16, 1081–1104. https://doi.org/10.5194/acp-16-1081-2016.

van Donkelaar, A., Martin, R.V., Brauer, M., Boys, B.L., 2015. Use of satellite observations for long-term exposure assessment of global concentrations of fine particulate matter. Environ. Health Perspect. 123 (2), 135–143. https://doi.org/10.1289/ehp.1408646.

Edenhofer, O., Elgizouli, I., Field, C.B., Howden, M., Pachauri, R.K., Meyer, L., Hallegatte France, S., Bank, W., Hegerl, G., Brinkman, S., van Kesteren, L., Leprince-Ringuet, N., van Boxmeer, F., Seyboth, K., 2014. IPCC. Available from: http://www.ipcc.ch. (Accessed 1 September 2018).

Evan, A.T., Flamant, C., Fiedler, S., Doherty, O., 2014. An analysis of aeolian dust in climate models. Geophys. Res. Lett. 41 (16), 5996–6001. https://doi.org/10.1002/2014GL060545.

Fortems-Cheiney, A., Foret, G., Siour, G., Vautard, R., Szopa, S., Dufour, G., Colette, A., Lacressonniere, G., Beekmann, M., 2017. A 3°C global RCP8.5 emission trajectory

cancels benefits of European emission reductions on air quality. Nat. Commun. 8, 1–6. https://doi.org/10.1038/s41467-017-00075-9.

Giorgi, F., 2006. Climate change hot-spots. Geophys. Res. Lett. 33 (8), 1–4. https://doi.org/10.1029/2006GL025734.

Griffin, D.W., 2007. Atmospheric movement of microorganisms in clouds of desert dust and implications for human health. Clin. Microbiol. Rev. 20 (3), 459–477. https://doi.org/10.1128/CMR.00039-06 table of contents.

Guenther, A., Karl, T., Harley, P., Wiedinmyer, C., Palmer, P.I., Geron3, C., 2006. Estimates of global terrestrial isoprene emissions using MEGAN (model of emissions of Gases and aerosols from nature). Atmos. Chem. Phys. 6, 3181–3210. https://doi.org/10.1016/j.cognition.2008.05.007.

Harrison, R.M., Yin, J., 2000. Particulate matter in the atmosphere: which particle properties are important for its effects on health? Sci. Total Environ. 249 (1–3), 85–101. Available from: http://www.ncbi.nlm.nih.gov/pubmed/10813449. (Accessed 30 May 2018).

Hauglustaine, D.A., Balkanski, Y., Schulz, M., 2014. A global model simulation of present and future nitrate aerosols and their direct radiative forcing of climate. Atmos. Chem. Phys. 14 (20), 11031–11063. https://doi.org/10.5194/acp-14-11031-2014.

Heald, C.I., Wilkinson, M.J., Monson, R.K., Alo, C.A., Wang, G., Guenther, A., 2009. Response of isoprene emission to ambient CO 2 changes and implications for global budgets. Global Change Biol. 15 (5), 1127–1140. https://doi.org/10.1111/j.1365-2486.2008.01802.x.

Israelevich, P., Ganor, E., Alpert, P., Kishcha, P., Stupp, A., 2012. Predominant transport paths of saharan dust over the Mediterranean Sea to Europe. J. Geophys. Res.: Atmosphere 117 (D2).

Jacob, D., Petersen, J., Eggert, B., Alias, A., Christensen, O.B., Bouwer, L.M., Braun, A., Colette, A., Déqué, M., Georgievski, G., Georgopoulou, E., Gobiet, A., Menut, L., Nikulin, G., Haensler, A., Hempelmann, N., Jones, C., Keuler, K., Kovats, S., Kröner, N., Kotlarski, S., Kriegsmann, A., Martin, E., van Meijgaard, E., Moseley, C., Pfeifer, S., Preuschmann, S., Radermacher, C., Radtke, K., Rechid, D., Rounsevell, M., Samuelsson, P., Somot, S., Soussana, J.-F., Teichmann, C., Valentini, R., Vautard, R., Weber, B., Yiou, P., 2014. EURO-CORDEX: new high-resolution climate change projections for European impact research. Reg. Environ. Change 14 (2), 563–578. https://doi.org/10.1007/s10113-013-0499-2.

Jacob, D.J., Winner, D.A., 2009. Effect of climate change on air quality. Atmos. Environ. 43 (1), 51–63. https://doi.org/10.1016/j.atmosenv.2008.09.051.

Jones, B., O'Neill, B.C., 2016. Spatially explicit global population scenarios consistent with the Shared Socioeconomic Pathways. Environ. Res. Lett. 11 (8), 084003 https://doi.org/10.1088/1748-9326/11/8/084003.

Kan, H., Chen, R., Tong, S., 2012. Ambient air pollution, climate change, and population health in China. Environ. Int. 42, 10–19. https://doi.org/10.1016/J.ENVINT.2011.03.003.

Klimont, Z., Kupiainen, K., Heyes, C., Purohit, P., Cofala, J., Rafaj, P., Borken-Kleefeld, J., Schöpp, W., 2017. Global anthropogenic emissions of particulate matter including black carbon. Atmos. Chem. Phys. 17 (14), 8681–8723. Available from: https://www.atmos-chem-phys.net/17/8681/2017/. (Accessed 23 May 2017).

Kuenen, J.J.P., Visschedijk, A.J.H., Jozwicka, M., Denier Van Der Gon, H.A.C., 2014. TNO-MACC-II emission inventory; A multi-year (2003-2009) consistent high-resolution European emission inventory for air quality modelling. Atmos. Chem. Phys. 14 (20), 10963–10976. https://doi.org/10.5194/acp-14-10963-2014.

LCSQA, 2015. Mise à disposition des AASQA de données de population spatialisée | LCSQA. Available from: https://www.lcsqa.org/fr/actualite/mise-dispositio n-aasqa-donnees-population-spatialisee. (Accessed 18 October 2018).

Lee, E.-H., Sohn, B.-J., 2011. Recent increasing trend in dust frequency over Mongolia and Inner Mongolia regions and its association with climate and surface condition change. Atmos. Environ. 45 (27), 4611–4616. https://doi.org/10.1016/J.ATMOSENV.2011.05.065.

Lelieveld, J., Lelieveld, J., Berresheim, H., Borrmann, S., Crutzen, P.J., Dentener, F.J., Fischer, H., Feichter, J., Flatau, P.J., Heland, J., 2002. Global Air Pollution Crossroads over the Mediterranean.Pdf, p. 794. https://doi.org/10.1126/science.1075457, 2002.

De Longueville, F., Hountondji, Y.-C., Henry, S., Ozer, P., 2010. What do we know about effects of desert dust on air quality and human health in West Africa compared to other regions? Sci. Total Environ. 409 (1), 1–8. https://doi.org/10.1016/J.SCITOTENV.2010.09.025.

Mahowald, N.M., Kloster, S., Engelstaedter, S., Moore, J.K., Mukhopadhyay, S., McConnell, J.R., Albani, S., Doney, S.C., Bhattacharya, A., Curran, M.A.J., Flanner, M.G., Hoffman, F.M., Lawrence, D.M., Lindsay, K., Mayewski, P.A., Neff, J., Rothenberg, D., Thomas, E., Thornton, P.E., Zender, C.S., 2010. Observed 20th century desert dust variability: impact on climate and biogeochemistry. Atmos. Chem. Phys. 10 (22), 10875–10893. https://doi.org/10.5194/acp-10-10875-2010.

Marticorena, B., Bergametti, G., 1995. Modeling the atmospheric dust cycle: 1. Design of a soil-derived dust emission scheme. J. Geophys. Res. 100 (D8), 16415. https://doi.org/10.1029/95JD00690.

Mauderly, J.L., Chow, J.C., 2008. Health effects of organic aerosols. Inhal. Toxicol. 20, 257–288. https://doi.org/10.1080/08958370701866008.

Meinshausen, M., Smith, S.J., Calvin, K., Daniel, J.S., Kainuma, M.L.T., Lamarque, J.-F., Matsumoto, K., Montzka, S.A., Raper, S.C.B., Riahi, K., Thomson, A., Velders, G.J.M., van Vuuren, D.P.P., 2011. The RCP greenhouse gas concentrations and their extensions from 1765 to 2300. Climatic Change 109 (1–2), 213–241. https://doi.org/10.1007/s10584-011-0156-z.

Menut, L., Schmechtig, C., Marticorena, B., 2005. Sensitivity of the sandblasting flux calculations to the soil size distribution accuracy. J. Atmos. Ocean. Technol. 22 (12), 1875–1884.

Menut, L., Bessagnet, B., Khvorostyanov, D., Beekmann, M., Blond, N., Colette, A., Coll, I., Curci, G., Foret, G., Hodzic, A., Mailler, S., Meleux, F., Monge, J.-L., Pison, I.,

Siour, G., Turquety, S., Valari, M., Vautard, R., Vivanco, M.G., 2013. Chimere 2013: a model for regional atmospheric composition modelling. Geosci. Model Dev. (GMD) 6 (4), 981–1028. https://doi.org/10.5194/gmd-6-981-2013.

Middleton, N.J., 2017. Desert dust hazards: a global review. Aeolian Res 24, 53–63. https://doi.org/10.1016/J.AEOLIA.2016.12.001.

Mulitza, S., Heslop, D., Pittauerova, D., Fischer, H.W., Meyer, I., Stuut, J.-B., Zabel, M., Mollenhauer, G., Collins, J.A., Kuhnert, H., Schulz, M., 2010. Increase in African dust flux at the onset of commercial agriculture in the Sahel region. Nature 466 (7303), 226–228. https://doi.org/10.1038/nature09213.

O'Neill, B.C., Kriegler, E., Ebi, K.L., Kemp-Benedict, E., Riahi, K., Rothman, D.S., van Ruijven, B.J., van Vuuren, D.P., Birkmann, J., Kok, K., Levy, M., Solecki, W., 2017. The roads ahead: narratives for shared socioeconomic pathways describing world futures in the 21st century. Global Environ. Change 42, 169–180. https://doi.org/10.1016/j.gloenvcha.2015.01.004.

Péré, J.-C., Pont, V., Mallet, M., Bessagnet, B., 2009. Mapping of PM10 surface concentrations derived from satellite observations of aerosol optical thickness over South-Eastern France. Atmos. Res. 91 (1), 1–8. https://doi.org/10.1016/J.ATMOSRES.2008.05.001.

Pope, C.A., Dockery, D.W., 2006. Health effects of fine particulate air pollution: lines that connect. J. Air Waste Manag. Assoc. 56 (6), 709–742. https://doi.org/10.1080/10473289.2006.10464485.

Riahi, K., Rao, S., Krey, V., Cho, C., Chirkov, V., Fischer, G., Kindermann, G., Nakicenovic, N., Rafaj, P., 2011. Rcp 8.5—a scenario of comparatively high greenhouse gas emissions. Climatic Change 109 (1–2), 33–57. https://doi.org/10.1007/s10584-011-0149-y.

Riahi, K., van Vuuren, D.P., Kriegler, E., Edmonds, J., O'Neill, B.C., Fujimori, S., Bauer, N., Calvin, K., Dellink, R., Fricko, O., Lutz, W., Popp, A., Cuaresma, J.C., Kc, S., Leimbach, M., Jiang, L., Kram, T., Rao, S., Emmerling, J., Ebi, K., Hasegawa, T., Havlik, P., Humpenöder, F., Da Silva, L.A., Smith, S., Stehfest, E., Bosetti, V., Eom, J., Gernaat, D., Masui, T., Rogelj, J., Strefler, J., Drouet, L., Krey, V., Luderer, G., Harmsen, M., Takahashi, K., Baumstark, L., Doelman, J.C., Kainuma, M., Klimont, Z., Marangoni, G., Lotze-Campen, H., Obersteiner, M., Tabeau, A., Tavoni, M., 2017. The Shared Socioeconomic Pathways and their energy, land use, and greenhouse gas emissions implications: an overview. Global Environ. Change 42, 153–168. https://doi.org/10.1016/j.gloenvcha.2016.05.009.

Robinson, A.L., Donahue, N.M., Shrivastava, M.K., Weitkamp, E.A., Sage, A.M., Grieshop, A.P., Lane, T.E., Pierce, J.R., Pandis, S.N., 2007. Rethinking organic aerosols: semivolatile emissions and photochemical aging. Science (80-.) 315 (5816), 1259–1262. https://doi.org/10.1126/science.1133061.

Samoli, E., Stafoggia, M., Rodopoulou, S., Ostro, B., Declercq, C., Alessandrini, E., Díaz, J., Karanasiou, A., Kelessis, A.G., Le Tertre, A., Pandolfi, P., Randi, G., Scarinzi, C., Zauli-Sajani, S., Katsouyanni, K., Forastiere, F., MED-PARTICLES Study Group, the M.-P. S., 2013. Associations between fine and coarse particles and mortality in Mediterranean cities: results from the MED-PARTICLES project. Environ. Health Perspect. 121 (8), 932–938. https://doi.org/10.1289/ehp.1206124.

Seinfeld, J.H., Pandis, S.N., 2016. Atmospheric Chemistry and Physics : from Air Pollution to Climate Change.

Shrivastava, M., Zelenyuk, A., Imre, D., Easter, R., Beranek, J., Zaveri, R.A., Fast, J., 2013. Implications of low volatility SOA and gas-phase fragmentation reactions on SOA loadings and their spatial and temporal evolution in the atmosphere. J. Geophys. Res. Atmos. 118 (8), 3328–3342. https://doi.org/10.1002/jgrd.50160.

Shrivastava, M., Easter, R.C., Liu, X., Zelenyuk, A., Singh, B., Zhang, K., Ma, P., Chand, D., Ghan, S., Jimenez, J.L., Zhang, Q., Fast, J., Rasch, P.J., Tiitta, P., 2015. Global transformation and fate of SOA: implications of low-volatility SOA and gas-phase fragmentation reactions. J. Geophys. Res. Atmos. 120 (9), 4169–4195. https://doi.org/10.1002/2014JD022563.Received.

Sicard, P., Mangin, A., Hebel, P., Malléa, P., 2010. Detection and estimation trends linked to air quality and mortality on French Riviera over the 1990–2005 period. Sci. Total Environ. 408 (8), 1943–1950. https://doi.org/10.1016/J.SCITOTENV.2010.01.024.

Sicard, P., Lesne, O., Alexandre, N., Mangin, A., Collomp, R., 2011. Air quality trends and potential health effects – development of an aggregate risk index. Atmos. Environ. 45 (5), 1145–1153. https://doi.org/10.1016/J.ATMOSENV.2010.12.052.

Tai, A.P.K., Mickley, L.J., Heald, C.L., Wu, S., 2013. Effect of CO 2 inhibition on biogenic isoprene emission: implications for air quality under 2000 to 2050 changes in climate, vegetation, and land use. Geophys. Res. Lett. 40 (13), 3479–3483. https://doi.org/10.1002/grl.50650.

Tarín-Carrasco, P., Im, U., Geels, C., Palacios-Peña, L., Jiménez-Guerrero, P., 2021. Contribution of fine particulate matter to present and future premature mortality over Europe: a non-linear response. Environ. Int. 153, 106517. https://doi.org/10.1016/j.envint.2021.106517}.

Tegen, I., Werner, M., Harrison, S.P., Kohfeld, K.E., 2004. Relative importance of climate and land use in determining present and future global soil dust emission. Geophys. Res. Lett. 31 (5) https://doi.org/10.1029/2003GL019216 n/a-n/a.

Thomson, A.M., Calvin, K.V., Smith, S.J., Page Kyle, G., Volke, A., Patel, P., Delgado-Arias, S., Bond-Lamberty, B., Wise, M.A., Clarke, L.E., Edmonds, J.A., 2011. RCP4.5: a Pathway for Stabilization of Radiative Forcing by 2100. https://doi.org/10.1007/s10584-011-0151-4.

Vincent, J., Laurent, B., Losno, R., Bon Nguyen, E., Roullet, P., Sauvage, S., Chevaillier, S., Coddeville, P., Ouboulmane, N., di Sarra, A.G., Tovar-Sánchez, A., Sferlazzo, D., Massanet, A., Triquet, S., Morales Baquero, R., Fornier, M., Coursier, C., Desboeufs, K., Dulac, F., Bergametti, G., 2016. Variability of mineral dust deposition in the western Mediterranean basin and south-east of France. Atmos. Chem. Phys. 16 (14), 8749–8766. https://doi.org/10.5194/acp-16-8749-2016.

West, J.J., Smith, S.J., Silva, R.A., Naik, V., Zhang, Y., Adelman, Z., Fry, M.M., Anenberg, S., Horowitz, L.W., Lamarque, J.-F., 2013. Co-benefits of mitigating global greenhouse gas emissions for future air quality and human health. Nat. Clim. Change 3 (10), 885–889. https://doi.org/10.1038/nclimate2009.

Wilkinson, M.J., Monson, R.K., Trahan, N., Lee, S., Brown, E., Jackson, R.B., Polley, H. W., Fay, P.A., Fall, R., 2009. Leaf isoprene emission rate as a function of atmospheric CO2 concentration. Global Change Biol. 15 (5), 1189–1200. https://doi.org/10.1111/j.1365-2486.2008.01803.x.

Yao, L., Lu, N., Yao, L., Lu, N., 2014. Particulate matter pollution and population exposure assessment over mainland China in 2010 with remote sensing. Int. J. Environ. Res. Publ. Health 11 (5), 5241–5250. https://doi.org/10.3390/ijerph110505241.

Zender, C.S., Bian, H., Newman, D., 2003. Mineral dust entrainment and deposition (DEAD) model: description and 1990s dust climatology. J. Geophys. Res. 108 (D14), 4416. https://doi.org/10.1029/2002JD002775.

Update

Atmospheric Environment
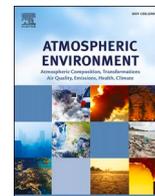
Corrigendum to "Exposure of the population of southern France to air pollutants in future climate case studies" [Atmos. Environ. 234 (2021) 118689]

Arineh Cholakian [a,b,c,*,1], Isabelle Coll [a], Augustin Colette [b], Matthias Beekmann [c]

[a] *Univ Paris Est Creteil and Université de Paris, CNRS, LISA, F-94010, Créteil, France*
[b] *Institut National de l'Environnement Industriel et des Risques, Parc Technologique ALATA, Verneuil-en-Halatte, France*
[c] *Université de Paris and Univ Paris Est Creteil, CNRS, LISA, F-75013, Paris, France*

The authors regret the wrong highlights were published for the paper. The corrected highlight section should be:

- Several future test cases have been explored for the south-eastern Mediterranean coasts of France.
- Simulations have been performed with the CHIMERE chemistry transport model.
- For each test case the appropriate anthropogenic emissions and future boundary/initial conditions have been taken into account for each time period.
- Meteorological parameters and species concentrations have been analysed.

- Population exposure on a general, individual and county-per-county level has been compared to a base test case using SSP scenarios.
- Exposure decreases on average for most species because of emission reduction policies, showing an increase for dust and BSOA in general, while ozone exposure increases only in urban areas.
- Three coastal counties might experience higher ozone, PM_{10} and $PM_{2.5}$, dust and BSOA exposure for the population.

The authors would like to apologise for any inconvenience caused.